DEVELOPING DEVICES AND TECHNIQUES FOR GLOBAL POINT-OF-CARE DIAGNOSIS OF INFECTIOUS DISEASE AND CANCER

A Dissertation

Presented to the Faculty of the Graduate School

of Cornell University

In Partial Fulfillment of the Requirements for the Degree of

Doctor of Philosophy

by

Duncan Scott McCloskey

August 2022

DEVELOPING DEVICES AND TECHNIQUES FOR GLOBAL POINT-OF-CARE DIAGNOSIS OF INFECTIOUS DISEASE AND CANCER

Duncan Scott McCloskey, Ph. D.

Cornell University 2022

One of the largest global healthcare challenges of the 21st century is improving access to adequate diagnostic testing, as emphasized by the SARS-COV-2 pandemic beginning in 2019. This is especially true in limited-resource settings where they lack the traditional healthcare infrastructure that is often necessary for rapid and accurate diagnosis, leaving countless patients undiagnosed and without proper treatment. Nucleic acid testing (NAT) is a molecular approach that can be used to diagnose a variety of pathogenic and genetic diseases through DNA quantification of a specific target, such as viral DNA, within a patient sample. Point-of-care (POC) application of NAT technologies can have powerful impacts globally, but perhaps most significantly in limited-resource settings where deployment of novel devices and methods in a decentralized setting can potentially out-pace the development of traditional healthcare infrastructure.

This dissertation details the development of three unique technologies to improve access to rapid and accurate diagnosis through NAT at the point-of-care. The second chapter describes a novel approach to diagnose a viral-borne skin cancer – Kaposi's sarcoma (KS) – using a POC device, TINY. The third chapter describes an extension of our goal for accessible NAT testing as we describe the development of a high-throughput device for COVID-19 testing, capable of hundreds of samples per day. The fourth chapter will discuss a novel POC device for the rapid extraction of DNA

from skin tissue biopsies, further enhancing the POC impact of molecular KS-diagnosis described in the second chapter. All three chapters detail developments for enabling rapid and accurate nucleic acid diagnosis, especially in limited-resource settings, through novel devices and techniques that can be applied at the point-of-care.

BIOGRAPHICAL SKETCH

Duncan grew up on Long Island in New York. He received his Bachelor of Science degree in nanoscale engineering from the Colleges of Nanoscale Science and Engineering within the University at Albany, where he was awarded a four-year fellowship for academic merit. Duncan began research on a DNA-hybridization biosensor for Lyme disease in the lab of Professor Nathaniel Cady, where his passion for research grew and he decided to pursue graduate school. At Cornell University he joined the lab of Professor David Erickson where he worked on translational engineering projects for point-of-care disease diagnosis. Duncan enjoys his time outside of research working on his car, woodworking, taking care of his ornamental shrimp, and unsuccessfully fishing. After graduation, Duncan will be moving with his wife and pets to Tennessee where he will work in medical affairs for a pharmaceutical company.

Dedicated to my loving wife, Samantha, and our three pets – Gunner, Taz, and Odin.

ACKNOWLEDGMENTS

I would like to thank all the people whose support has enabled my success thus far.

I would like to thank my advisor, David Erickson, for his continued mentorship throughout my time at Cornell. David was always insightful, provided guidance and structure when I needed it, yet gave me his trust and the freedom to find solutions on my own. I have been able to grow personally and professionally thanks to the opportunities that working with David has provided and I feel very fortunate.

Additional thanks to my special committee members, Robert Shepherd and Saurabh Mehta, for their insight and guidance along the way. I would like to thank my undergraduate advisor Nathaniel Cady for encouraging me to pursue graduate studies at Cornell. I would also like to thank my collaborators across the US and in Africa, as well as the National Cancer Institute for supporting my research.

Thank you to current and former members of the Erickson lab for the insights and assistance over the past five years. Special thanks to Ryan Snodgrass and Juan Boza for their direct contributions to my research.

Thank you to my family for always encouraging me and supporting me throughout my education. Thanks to my brother, Angus, for making me laugh and teaching me to relax more. Thanks to my pets Gunner, Taz, and Odin for being such good boys.

Finally, I would like to thank my wife, Samantha, for her unwavering support and love through the years. You help me every day to become a better version of myself.

TABLE OF CONTENTS

LIST OF FIGURES

LIST OF TABLES

LIST OF ABBREVIATIONS

ART – anti-retroviral therapy

AUC – area under the curve

CI – confidence interval

H&E – hematoxylin and eosin

HHV-8 – human herpesvirus 8

HPV – human papillomavirus

KS – Kaposi's sarcoma

KSHV – Kaposi's sarcoma -associated herpesvirus

LAMP – loop-mediated isothermal amplification

LANA – latency-associated nuclear antigen

LED – light emitting diode

NAT – nucleic acid testing

NC – negative control

PC – positive control

PCB – printed circuit board

PCM – phase change material

PD – photodiode

POC – point-of-care

qPCR – quantitative polymerase chain reaction

ROC – receiver operating characteristic

RPM – revolutions per minute

CHAPTER 1

INTRODUCTION

1.1 Overview

One of the most pressing challenges for global health is to increase access to rapid and accurate diagnostic technologies. This is especially true in limited-resource settings where access to traditional healthcare infrastructure is limited. Point-of-care approaches can be used to reduce reliance on hospital or laboratory diagnosis and have increased impact in limited-resource settings where decentralized healthcare is common. Nucleic acid-based testing is a common laboratory technique for the diagnosis or screening of various diseases and can be especially powerful when employed in a point-of-care format such that patients can be tested a local clinic or community center instead of a hospital or diagnostic laboratory.

Detailed within this dissertation, we have developed multiple devices and techniques to meet the need for point-of-care accessible nucleic acid diagnostics. The largest focus of this work revolves around increasing the accuracy and availability of diagnosis for patients in sub-Saharan Africa who are clinically suspected as having a skin cancer, Kaposi's sarcoma. Chapter 2 and Chapter 4 are directly related to development of a novel approach that can be used at the point-of-care, increasing access to timely diagnosis and therapy through reduced reliance on the limited infrastructure for traditional pathologic diagnosis. Chapter 3 is an extension of this overall effort towards accessible diagnostics, with an emphasis on high-throughput testing.

1.2 Molecular Approach for Kaposi's Sarcoma Diagnosis

Chapter 2 details the development of a novel approach for molecular diagnosis of a dermatological cancer, Kaposi's sarcoma, which has high incidence and poor survivability in sub-Saharan Africa. The reason for poor survival is multifactorial but can largely be attributed to the lack of accurate and timely diagnosis due to limited pathology infrastructure, leading to the majority of patient diagnoses occurring at advanced-stage disease. Our approach utilizes loop-mediated isothermal amplification to quantify the amount of cancer-causing virus – Kaposi's sarcoma-associated herpesvirus – from within clinically suspected lesion biopsies. Utilizing a point-of-care device previously developed within our group, TINY, which was designed for use in limited-resource settings, we are able to achieve molecular diagnosis of KS with 96% accuracy compared to gold standard US-based pathology. This effort was validated on over 500 patient biopsies from three separate clinics in Uganda. The results detailed within could be particularly transformative to diagnosis of this cancer, and similar diseases, within limited-resource settings where decentralized healthcare is common. Reducing the barriers to obtaining KS diagnosis and improving the accuracy of the result could enable earlier diagnosis and subsequent initiation of treatment, improving health outcomes and overall survivability of this disease.

1.3 High-throughput Device for Nucleic Acid Testing

Chapter 3 details the development of a nucleic acid testing device capable of analyzing 96 samples simultaneously, and potentially hundreds of samples per day. The SARS-COV-2 pandemic that began in 2019 emphasized the need for high-throughput devices capable of testing very large numbers of patients each day, when even high-resource nations initially struggled to meet the demand for rapid nucleic acid testing. Due to the success of our efforts in Chapter 2, we sought to extend the impact of our point-of-care technologies for high-throughput testing. Our device, MINI, maintains the portability, energy-flexibility, robust construction, and operational simplicity of previous devices in our lab while greatly increasing the testing capacity. In this chapter we will discuss the challenges of expanding to a 96-sample format within a small device, and the novel design features to enable high-resolution testing with minimal device footprint and electronic requirements. Overall, MINI achieves very consistent amplification and optical isolation throughout the 96 wells of the device and can produce comparable amplification performance to a commercially available instrument, while maintaining unique point-of-care features such as solar-heating and ~90 minutes of run-time without electricity. Future directions for this device could also include tuberculosis testing or cervical cancer screening for limited-resource settings.

1.4 Rapid DNA Extraction from Tissue Biopsies

Chapter 4 details the development of a device for rapid nucleic acid extraction from tissue biopsies, as an effort to maximize the impact of the results from Chapter 2. Nucleic acid extraction is often the rate-limiting step of many sample processing protocols, especially for large, physically robust sample types such as the skin lesion biopsies we are using for KS diagnosis. With purified nucleic acids, our approach from Chapter 2 can be performed in under an hour. However, the extraction of nucleic acids from skin biopsies takes about 4 hours with an attentive operator performing regular mixing using a standard commercially available extraction kit. Frequently, operators are not available for regular mixing and the extraction step takes significantly longer, often requiring an overnight incubation and testing the following day. To reduce the time requirement for complete DNA extraction we have developed a device, BLENDER, for the simultaneous homogenization and enzymatic digestion of tissue. Using 3D-printed parts and inexpensive electronics, BLENDER combines the effectiveness of large, expensive commercial homogenizers with the DNA extraction performance of heated enzymatic lysis all within a single, small device. Our approach is able to produce a complete DNA yield from a 3mm skin biopsy in only 15 minutes with no negative effects on downstream amplification for diagnostic testing. Decreasing the sample processing time for molecular KS diagnosis, with carryover to other dermatological and solid-tissue testing, could decrease time-to-result for downstream analysis, enabling faster point-of-care diagnosis and subsequent initiation of treatment in limited resource settings.

CHAPTER 2

LAMP-ENABLED DIAGNOSIS OF KAPOSI'S SARCOMA FOR SUB-SAHARAN AFRICA*

2.1 Abstract

Kaposi's sarcoma (KS) is a cancer of endothelial origin caused by the Kaposi's sarcoma-associated herpesvirus (KSHV) and is one of the most common cancers in sub-Saharan Africa. Timely KS diagnosis is particularly difficult in limited resource settings where infrastructure for traditional pathology diagnosis is insufficient. Therefore, diagnosis of KS often occurs at advanced-stage where survival is poor. In this study, we investigate loop-mediated isothermal amplification (LAMP)-enabled molecular diagnosis of KS that can be performed in a point-of-care device to circumvent the limited infrastructure for traditional diagnosis. Using 506 mucocutaneous biopsies collected from patients at 3 HIV clinics in Uganda, we achieved 97% sensitivity, 92% specificity, and 96% accuracy compared to gold standard US-based pathology. To our knowledge, this is the first demonstration that LAMP-based quantification of KSHV DNA extracted from KS-suspected biopsies can serve as a successful diagnostic for the disease and that diagnosis can be accurately achieved using a point-of-care device. Reducing the barriers to obtaining KS diagnosis while increasing the accuracy of the result could enable earlier diagnosis and subsequent treatment, improving health outcomes and overall survivability.

*This work by Duncan McCloskey and David Erickson *et al.* was undergoing peer-review for publication in *Science Advances* as of June 2022.

2.2 Introduction

Kaposi's sarcoma (KS) is a cancer of lymphatic endothelial origin caused by the Kaposi's sarcoma-associated herpesvirus (KSHV; also known as human herpesvirus 8 (HHV-8)) [1-4]. It is one of the most common and deadly cancers in sub-Saharan Africa where its development is frequently driven by immune suppression from HIV infection [5, 6]. Treatment for KS entails use of anti-retroviral therapy (ART) and chemotherapeutics with recovery significantly more likely when a diagnosis is obtained and therapies administered in the early-stages of the disease [7]. Survival however is still poor for most patients in sub-Saharan Africa as the disease is often not diagnosed until it is at an advanced stage [8-14]. A population-based estimate found that 82% of newly diagnosed KS patients are classified as T1 advanced disease by AIDS Clinical Trials Group criteria [15]. Patients diagnosed at this stage have between a 2.7 to 7.4-fold greater chance of death than those at the T0 stage [16-19].

The reason for persistent late-stage diagnosis of KS is multifactorial but is at least partially due to the lack of local capacity for traditional pathologic diagnosis. KS typically presents with non-specific dark lesions on the skin or mucous membranes and clinical diagnosis is often made based on the macroscopic appearance of these lesions, where they can be confused with other common skin conditions. In a study analyzing 739 East African patients referred with lesions suspicious for KS, only 77% of clinical diagnoses were found to be accurate after review by U.S. pathologists [20]. Therefore, clinical suspicion alone is suboptimal, and a more objective diagnostic test is needed. The typical alternative is pathologic diagnosis, but an assessment of local pathology revealed a sensitivity of 72% and a specificity of 84% when compared to gold standard

analysis [20, 21]. This challenge is compounded by the scarcity of trained pathologists, as almost all sub-Saharan African countries have fewer than one for every 500,000 people [22]. Where pathologists are available, patients must return for a second visit to receive results and turnaround time is often extensive, all resulting in delays in receiving diagnosis and subsequent therapy [23].

To address the issue of late-stage diagnosis, we hypothesized that a rapid point-of-care diagnostic test for KS could be developed by taking advantage of the viral nature of the disease and quantifying the amount of KSHV DNA from a KS-suspected mucocutaneous lesion biopsy. Qualitative testing only for the presence of KSHV infection would not work due to the endemic nature of the virus, with between 30% to 60% seroprevalence in sub-Saharan Africa [24]. However, quantification of the viral load within suspected KS lesions could offer much higher specificity that would be needed for an accurate diagnostic test. Point-of-care tests based on nucleic acid detection have proven successful at decreasing time to diagnosis and improving outcomes for infectious disease [25-28] but there have been few attempts to apply similar methodologies to cancers. To our knowledge there is no prior evidence of successful nucleic acid based testing for the diagnosis of KS [29].

Here, we present the results of LAMP (Loop-Mediated Isothermal Amplification)-based molecular diagnosis of KS using nucleic acid extracted from skin lesion biopsies collected from 506 patients from three different HIV clinics in Uganda. The analysis is conducted in TINY (Tiny Isothermal Nucleic acid quantification sYstem) a portable and energy-flexible point-of-care device which we have demonstrated [30] is compatible with the requirements for operation in limited resource

settings [31-34]. This represents the first large-scale effort to determine both if LAMP-based nucleic acid quantification can accurately diagnose KS and to conduct that analysis in a point-of-care compatible device. For all samples, a portion of the tissue was used for local standard-of-care pathology to guide clinical treatments. Molecular analysis and gold standard pathology were performed in the U.S. in order to reduce the number of confounding variables.

2.3 Results

We consecutively consented and collected 506 patient biopsies across three different clinics in Uganda in order to test whether the LAMP-based approach could be a feasible alternative to traditional histopathology methods (Figure 2.1). Standard care for patients who present with lesions clinically suspected of being KS includes a biopsy that is sent for pathology analysis. This traditional approach has significant associated costs due to the scarcity of skilled pathologists and limited availability of resources. Our proposed alternative is to apply modern molecular techniques by extracting and purifying viral DNA from the tissue, which can then be quantified using LAMP in order to offer a more timely and inexpensive diagnosis.

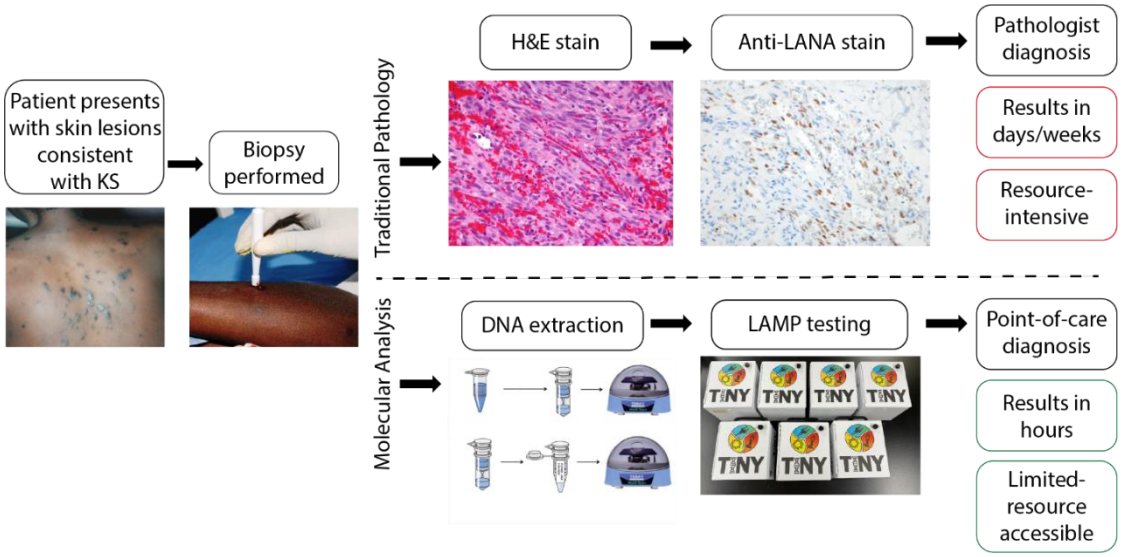

Figure 2.1 – Flow diagram for traditional and proposed diagnosis techniques. Comparison of traditional histopathologic diagnosis of KS and proposed molecular diagnostic method. After clinical examination and biopsy, traditional diagnosis is performed using an H&E stain and an anti-LANA stain if available. This is considered the gold standard for KS diagnosis yet is resource demanding. Molecular analysis using skin requires DNA extraction and purification prior to LAMP testing in TINY. This point-of-care approach may provide a diagnosis in only a few hours, as well as be accessible within limited-resource settings.

2.3.1 Parallel tissue analysis using histopathology and LAMP

To assess the efficacy of LAMP as a KS diagnostic tool, we analyzed each patient sample using two techniques. Tissue samples received a diagnosis using (1) gold standard US-based histopathology and (2) molecular analysis using LAMP (Figure 2.2). Biopsies were collected in Uganda, with a portion used for local care, and the remaining portion shipped to the United States for both pathology and molecular analyses.

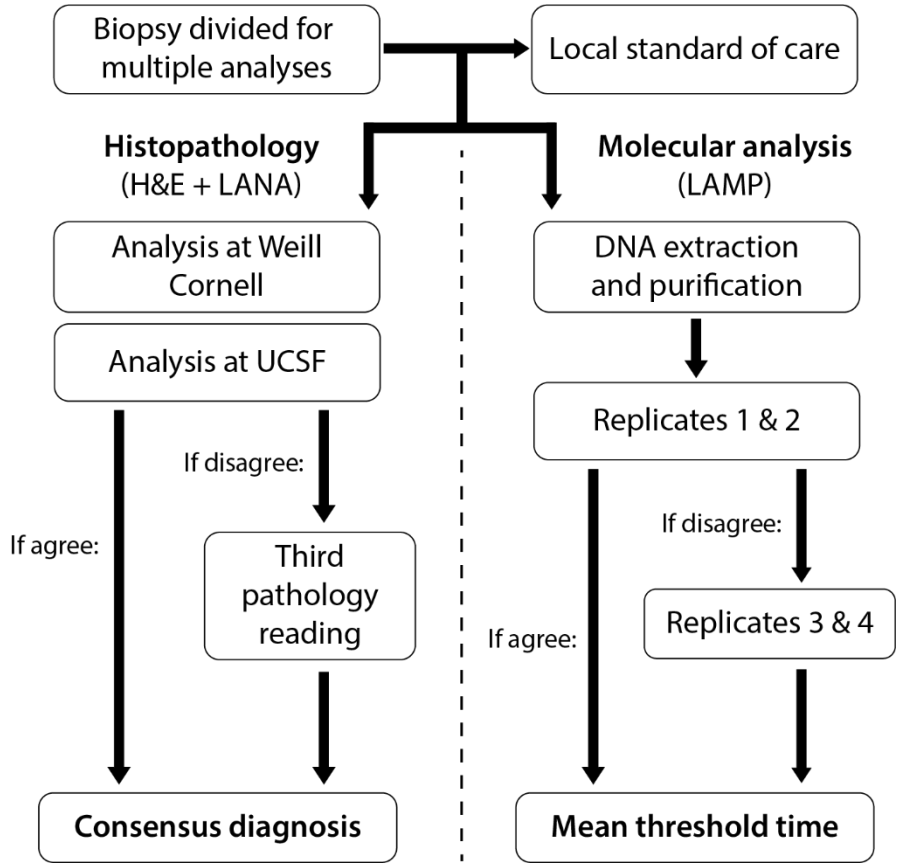

Figure 2.2 – Study design flow for biopsy analysis. Study design for analysis of LAMP as a diagnostic tool for KS. A section of biopsy is sent for analysis by at least two U.S. pathologists, where a third pathologist is used if a consensus diagnosis is not made. A different portion of the biopsy undergoes DNA extraction and purification prior to being tested in duplicate in the TINY. If those replicates disagree – one did not amplify and the other did, or they are among the top 5% of disparate threshold times – then additional replicates are performed. The output value used for KS diagnosis is the mean threshold time of all available (two or four total) replicates.

Traditional diagnosis begins with hematoxylin and eosin (H&E) staining, which was performed in Uganda. Immunohistochemistry for KSHV latency-associated nuclear antigen (LANA) was performed at Weill Cornell Medicine, where a blinded pathologic assessment for presence vs. absence of KS was conducted. This was followed by a second assessment by a dermatopathologist at the University of California, San Francisco. If the two pathology readings were in agreement, then a consensus diagnosis was rendered positive for KS, negative for KS, or indeterminate. An indeterminate result could result from either insufficient or inadequately processed tissue, as well as tissue with some but not all features of KS in combination with a negative or unconvincing LANA stain. Given a disagreement or indeterminate consensus, a third reading by an additional pathologist was conducted. The consensus diagnosis of positive or negative for KS was then made if two of the three readings agreed, where a result of indeterminate could mean the consensus was indeterminate or there was no consensus.

Concurrent to the pathology readings, molecular analysis of a biopsy section was performed by quantifying the amount of KSHV present using LAMP. Total DNA was extracted from the tissue and purified using the QIAGEN DNeasy Blood & Tissue kit. Amplification was performed in the point-of-care LAMP device TINY while targeting the *Orf26* gene of KSHV (Figure A.1). Part of our hypothesis is that lesions diagnosed positive for KS should exhibit large amounts of KSHV present within the biopsy. Therefore, strong KSHV amplification would likely indicate a positive KS diagnosis. Conversely, weak or no amplification would likely indicate a negative KS diagnosis. Samples were tested in duplicate and classified according to their mean amplification threshold time. Since LAMP does not operate using temperature cycles like in qPCR,

the amplification threshold time for our LAMP reaction signifies the point, measured in minutes, at which amplification overcomes our threshold for random noise. Samples were tested again in duplicate if their threshold times disagreed – one sample amplified and one did not, or the disparity between replicates was greater than 2 minutes 40 seconds (top 5%).

2.3.2 Reproducibility of LAMP threshold times during KSHV analysis

All 506 patient samples were analyzed according to the study design described in Figure 2. Initial LAMP analysis produced two threshold times for each patient sample. A Bland-Altman plot was used to visualize the concordance between the first two replicates for each patient when both replicates amplified (Figure 2.3). A large majority of the samples had a threshold difference of less than 2 minutes, especially at earlier time points (n=460). Lower amounts of KSHV present produced later amplification times, which is less consistent in our LAMP assay [30]. Samples that were in the top 5% of threshold time difference had a disparity of 2 minutes 40 seconds or greater and were re-tested in duplicate (n=18). Additionally, samples where one replicate did not amplify and one replicate saw positive amplification also had third and fourth replicates completed (n=28). The Bland-Altman coefficient of repeatability for samples with mean threshold times under 20 minutes was 1 minute 55 seconds (n=325). Samples with later threshold times had a larger repeatability coefficient due to lower copy numbers causing later amplification that was less consistent.

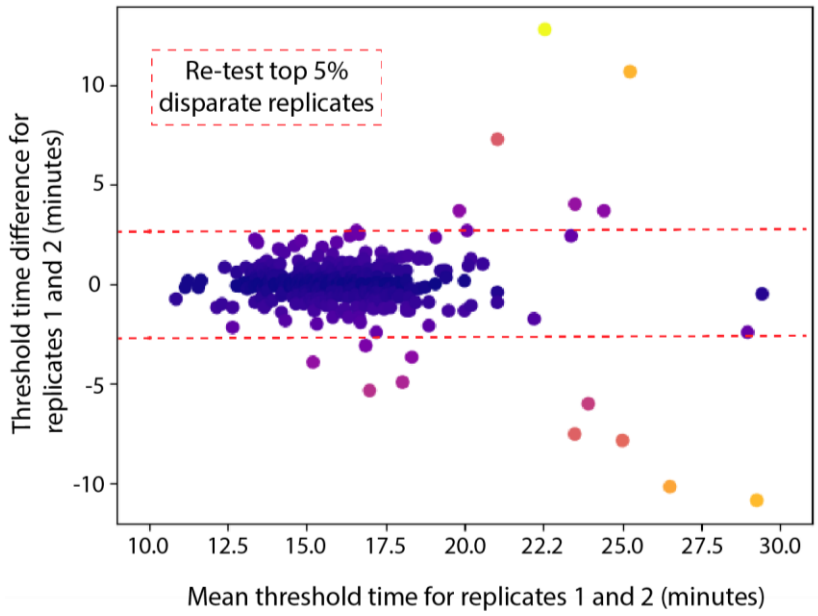

Figure 2.3 – Multi-replicate KSHV-LAMP reproducibility analysis. A Bland-Altman plot (n=356) of LAMP replicates 1 and 2 when both amplified. Dashed lines exclude replicates (n=18) with top 5% largest difference (absolute threshold time difference of 2 minutes 40 seconds and greater) to be re-tested in duplicate. Darker data point color indicates a difference closer to zero.

2.3.3 Performance of LAMP as a KS diagnostic method

Overall, KS diagnosis using LAMP shows very good agreement with gold standard pathology diagnosis. Comparison of LAMP threshold times with the consensus pathology result shows samples with early threshold times are highly likely to be reported KS-present by pathology while KS-negative samples are most often not amplifying at all (Figure 2.4). A large majority of the KS-present samples as indicated by the consensus pathology result had mean threshold times between 12 and 22 minutes, while KS-absent samples often had threshold times of 50 minutes, indicating that no amplification was detected throughout the duration of the assay.

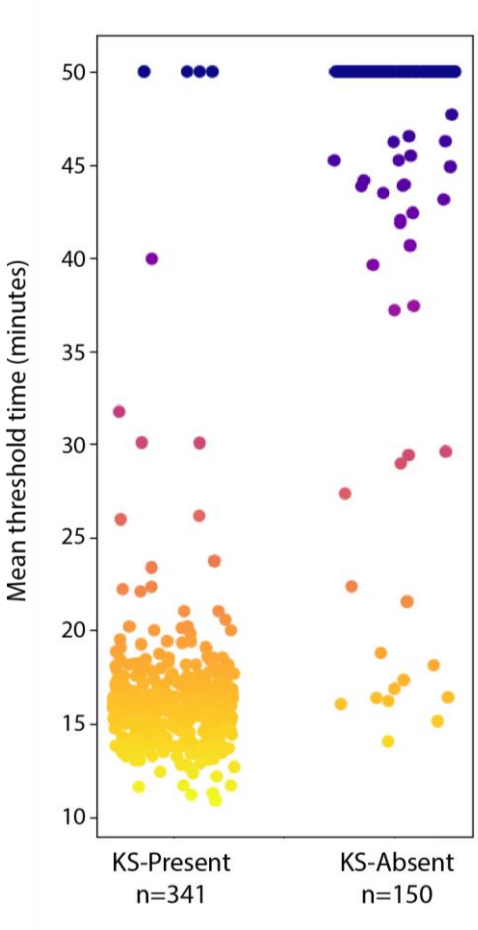

Figure 2.4 – Threshold time comparison of KS-Present and KS-Absent samples. Mean KS-LAMP threshold time value for all available replicates organized by consensus pathology result; mean of two replicates used for n=448, mean of four replicates used for n=43. Excluding samples indeterminate by pathology (n=15). Darker color indicates later threshold time.

A receiver operating characteristic (ROC) curve is used to illustrate the efficacy of LAMP as a diagnostic method for KS (Figure 2.5). The area-under-the-curve (AUC) was 0.967 with a 95% confidence interval (CI): 0.948-0.985. Two cutoff times were selected to maximize either sensitivity or specificity of the assay, while keeping 90% as the minimum for the non-maximized value. At 18 minutes 45 seconds, specificity is optimized at 94% with a sensitivity of 90%. This cutoff produces an overall accuracy of 91% when using the mean of all available replicates. A cutoff time of 26 minutes 10

seconds optimizes the sensitivity of the assay at 97% while maintaining a specificity of 92%, producing an overall accuracy of 96%.

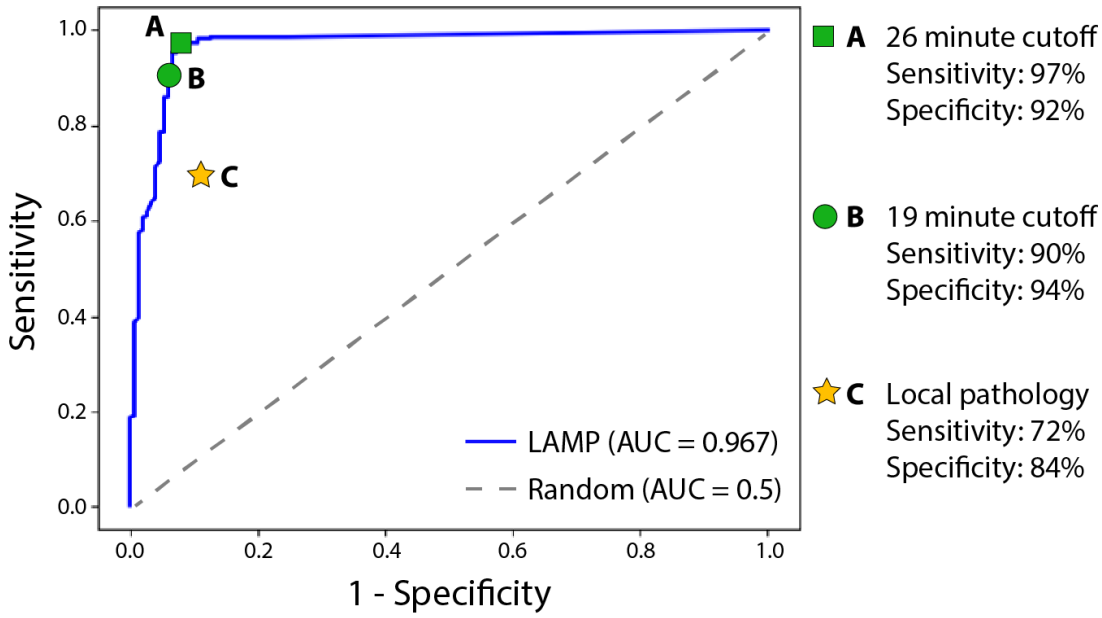

Figure 2.5 – Diagnostic performance of KSHV-LAMP. An ROC curve was generated from the sensitivity and specificity results for each cutoff time through the range of all possible values. The AUC was 0.967 (95% CI: 0.948-0.985) with two cutoff times shown at maximum sensitivity or specificity while keeping the other above 90%. Local pathology had a reported 72% sensitivity and 84% specificity[21].

For generating the ROC curve, we introduced a cutoff time for the threshold values (Figure A.2). At a given cutoff time *t*, any samples with a mean threshold time value prior to the cutoff would be considered a KS-positive diagnosis by the LAMP assay. Similarly, samples with a mean threshold time value after the cutoff would be considered KS-negative. Each cutoff value produces a sensitivity and specificity result when compared to the known true diagnosis from the pathology classification. An ROC is generated using the cumulative sensitivity and specificity results as the cutoff time *t* is moved through the range of available times.

2.4 Discussion

Kaposi's sarcoma has a high disease burden in sub-Saharan Africa where there is limited infrastructure for traditional pathology, making timely diagnosis difficult. Our goal was to assess the performance of LAMP-based biopsy analysis as a new approach to diagnose KS at the point-of-care. With biopsies collected from Ugandan patients suspected of having KS, we compared our molecular approach to gold standard US-based histopathology. Analysis of 506 biopsies shows that we are able to diagnose KS with an accuracy of 96%, a sensitivity of 97%, and a specificity of 92%, exceeding the accuracy of clinical suspicion and local pathology [20, 21]. The impact of our approach is further amplified by the fact that diagnosis is accomplished using a point-of-care device that can give an accurate result with minimal training, equipment, and consumables required[30].

With success of LAMP and the TINY in our US-based laboratory setting, the continuation of this effort will include deployment and testing at several sites across sub-Saharan Africa. One of the limitations of this study is the fact that all molecular testing was performed in pristine laboratory conditions with a highly trained US operator. In order to assess the real-world performance of our approach with local testing in real-time, where issues like contamination could affect overall diagnostic performance, we will expand to several sites across sub-Saharan Africa.

Molecular approaches for screening of cancer and other skin conditions can offer the possibility of earlier diagnosis compared to traditional approaches[35, 36], especially in limited resource settings [37, 38]. Our LAMP-based approach for KS can provide an

accurate diagnosis after only a few hours compared to the days to weeks that patients wait for a pathology diagnosis [30]. This reduced time-to-result could enable faster initiation of accurate treatment, improving patient outcomes. Eliminating the long wait time for a biopsy result could also eliminate the risk of inaccurate treatment, such as prescribing dangerous chemotherapeutics to a KS-negative patient. With continued improvement, molecular analysis could be the first step for future KS diagnosis, where assessment by a pathologist is only needed in borderline or unclear cases. Additionally, advancements in point-of-care technologies should continue to reduce testing costs, increase testing capacity, and simplify the user training required.

While our immediate focus is on KS diagnosis, the use of LAMP and other forms of isothermal amplification can be adapted for similar dermatological diseases [39, 40]. Skin-associated infections of various organisms – viral, mycobacterial, and fungal – can all cause conditions where immunohistochemistry or microbiologic culture is needed for diagnosis [39, 41, 42]. Even in settings with plentiful resources, diagnosis of certain conditions can be difficult [43], making a definitive diagnosis extremely rare in limited resource settings. It is also unlikely that sufficient immunohistochemistry and culture capability will become common in developing nations before nucleic acid testing devices become widely available. Clinical adoption of nucleic acid testing in limited resource countries has already been successful with certain diseases, such as using the GeneXpert for tuberculosis testing [25]. Future advancements in sample processing technologies could also reduce the time and processing steps required prior to molecular analysis. As such, point of care devices with broad applications in this testing domain should become exceedingly useful as assays are developed for more skin diseases.

2.5 Materials and Methods

2.5.1 Experimental Design

We consented and enrolled Ugandan patients presenting to clinics with skin lesions that were clinically consistent with KS. These patients were enrolled from various clinics in Uganda that included: The Infectious Diseases Institute (IDI) clinic in Kampala; all Kampala City Council Authority (KCCA) clinics that provide HIV care and which are supported by the IDI; Mbarara University Immune Suppression Syndrome (ISS) Clinic in Mbarara; and the Uganda Cares HIV clinic located at the Masaka Regional Referral Hospital in Masaka. Informed consent was obtained after the nature and possible consequences of the study was explained. All research was granted regulatory approval in the United States and Uganda.

2.5.2 Biopsy removal and preparation

Longitudinal skin punch biopsies were taken using a 5mm cylindrical punch biopsy tool on skin lesions consistent with KS morphology. Following removal, biopsies were longitudinally sectioned into two pieces. One half of the biopsy was immediately placed in 10% neutral buffered formalin (NBF) and processed for histopathology analysis, while the other half was stored in RNAlater for KSHV DNA analysis and subsequently frozen at -80°C.

2.5.3 Histopathology preparation and diagnosis

The portion of the biopsy designated for histopathology was placed in 10% NBF for no more than 24 hrs, and processed using routine procedures for paraffin embedding. This

was performed at the Pathology Department of Makerere University, Kampala, Uganda. For each patient, blocks were sent to Weill Cornell Medicine Department of Pathology and Laboratory Medicine, where immunohistochemistry for KSHV LANA was performed on a Leica Bond III system. Sections were pre-treated using heat-mediated antigen retrieval with Sodium-Citrate buffer (pH6, epitope retrieval solution 1) for 30 mins. The sections were then incubated with anti-LANA rat monoclonal HHV-8 ORF72 clone LN53 (Abcam) for 15 mins at room temperature and detected using an HRP-conjugated compact polymer system. 3,3'-Diaminobenzidine (DAB) was used as the chromogen. Sections were then counterstained with hematoxylin and mounted with micromount. Histology (H&E) and immunohistochemistry was reviewed in a blinded fashion by two pathologists.

2.5.4 DNA extraction and purification

One quarter of the stored biopsy tissue in RNAlater underwent DNA extraction and purification using the DNeasy Blood & Tissue kit (QIAGEN). Samples weighing around 10mg on average were incubated with 20 µl proteinase K and 180 µl ATL buffer until completely clear according to protocol, often taking 1-3 hours with intermittent vortexing. Once clear, 200 µl of AL buffer was added, samples were vortexed and then incubated for 10 minutes at 56°C. After incubation, 200 µl of 200 proof ethanol was added and samples were vortexed. Two wash steps were performed using the DNeasy spin columns and AW1/AW2 buffers to remove any potential remaining contaminants. The DNA was eluted into 75µL of AE buffer after one minute of the buffer soaking the

membrane at room temperature. Purified DNA was then measured using NanoDrop and diluted to a final concentration of 2ng/µl for analysis in TINY.

2.5.5 LAMP assay for KSHV

Mastermix was created using Isothermal Amplification Buffer, dNTP mix, and $MgSO_4$ (all from New England Biolabs) as well as six LAMP primers for the target *Orf26* of KSHV. Approximately 101µl of this mastermix was aliquoted into individual 1.5µl Eppendorf tubes, enough for one test in TINY using all six wells (after addition of water, enzyme, and DNA). The exact composition of this mastermix can be found in our previous publication[30]. Before running a test in TINY, 104µl of DNase/RNase-free water was added to the 101µl of mastermix. Then 9.8µl of Bst 2.0 Warmstart polymerase (New England Biolabs) is added and gently vortexed to homogenize the complete mixture. 35µl of this final mixture is distributed to six 200µl PCR tubes and 5µl of DNA is added to each. Two tubes are reserved for positive and negative control DNA, while the other four tubes are used for testing sample DNA from two patients in duplicate.

2.5.6 Statistical analysis

A Bland-Altman plot was used to determine the reproducibility of TINY replicates [44]. Obtaining sensitivity and specificity values, as well as ROC curve generation and confidence interval determination, was performed using scikit-learn with Python 3.6.

2.6 Acknowledgements

We would like to acknowledge our extensive list of collaborators in the US and Africa for their efforts and contributions. Specifically, we would like to thank Jane Frances Nalubega, Priscilla Namaganda, Prossy Kyomuhangi from IDI; Haruna Semuwemba, Stella Nabunya, Dr. Charles Kasozi from Uganda Cares HIV clinic Masaka; and Bronia Mwine, Placidia Owembabazi, Martin Mwebesa, and the late Dr. Bosco Mwebesa Bwana at ISS Clinic Mbarara. This work was supported by National Institutes of Health/National Cancer Institute grant UH2/UH3CA202723.

CHAPTER 3

MINI: A HIGH-THROUGHPUT POINT-OF-CARE DEVICE FOR PERFORMING HUNDREDS OF NUCLEIC ACID TESTS PER DAY**

3.1 Abstract

There are a variety of infectious diseases with a high incidence and mortality in limited resource settings that could benefit from point of care molecular diagnosis. Global health efforts have sought to implement mass-screening programs to provide earlier detection and subsequent treatment in an effort to control transmission and improve health outcomes. However, many of the current diagnostic technologies under development are limited to fewer than 10 samples per run, which inherently restricts the screening throughput of these devices. We have developed a high throughput device called "MINI" that is capable of testing hundreds of samples per day at the point-of-care. MINI can utilize multiple energy sources – electricity, flame, or solar – to perform loop-mediated isothermal amplification in a portable yet robust device for use in limited resource settings. The unique opto-electronic design of MINI minimizes the energy and space requirements of the device and maximizes the optical isolation and signal clarity, enabling point-of-care analysis of 96 unique samples simultaneously with comparable performance to a commercial analyzer. With a single device capable of running hundreds of samples per day, increased access to modern molecular diagnostics could improve health outcomes for a variety of diseases common in limited resource settings.

**This work by Duncan McCloskey and David Erickson *et al.* is was submitted to Biosensors and Bioelectronics as of June 2022.

3.2 Introduction

Molecular diagnostic approaches can be very powerful tools for screening and diagnosing viral-borne diseases at the point-of-care (POC). POC testing and mass-screening efforts have shown success in quickly identifying illness and enabling rapid implementation of treatment and approaches to reduce transmission. The need for high-throughput diagnostic devices was emphasized by the SARS-COV-2 pandemic that began in 2019[45-47], however, there are numerous other diseases that would benefit from rapid molecular diagnosis[5, 48-53] . A high-throughput, POC device could enable large-scale screening in a decentralized format, limiting the burden on traditional healthcare infrastructure and reducing the time to result before treatment is administered[54, 55]. These benefits would be further evident in limited-resource settings that often do not have access to state-of-the-art laboratories or traditional healthcare facilities.

A gold standard laboratory approach for molecular diagnosis is the quantitative polymerase chain reaction (qPCR) which can be used to measure small amounts of nucleic acids (DNA or RNA) within a sample. These nucleic acids can serve as indicators for disease, either pathogenic or genetic in origin[56, 57]. However, conventional qPCR methods can be difficult to employ at the POC, particularly in limited-resource settings, due to the complexity of thermal cycling and cost of equipment[31, 58, 59]. Loop-mediated isothermal amplification (LAMP) is an alternative approach that offers additional benefits for POC testing, such as single-temperature operation and resistance to inhibitors[60-62]. A number of devices have been developed for implementing LAMP testing at the POC for infectious diseases like tuberculosis[25, 27], malaria[63, 64], and COVID-19[65-67], as well as for cancers including cervical cancer[68-71]

and Kaposi's sarcoma[30]. However, all of these technologies are lacking the high-throughput capability to analyze potentially hundreds of samples per day, which is necessary for successful mass-screening[30, 72]. Some approaches utilize smartphones and inexpensive electronics to perform optical measurements, but can only run up to 6 samples at a time[30, 67, 73, 74]. Microfluidic chips and paper-based platforms combined with an optical reader have also been developed, though similarly can only process single-digit samples per run[75-78]. While some groups claim the ability to multiplex for improved testing capacity, reliance on complicated microfluidic approaches or increasing the size of a device further reduces the accessibility at the point of care. There has been development of a mobile fluorescence reader capable of 96-sample analysis, however, this device does not perform LAMP and can only be used for post-reaction measurements[79].

Here, we introduce the first fully-integrated Multiplexed Isothermal Nucleic acid amplIfication device, MINI, for 96-sample high-throughput molecular diagnosis and screening at the point-of-care. MINI is capable of performing and processing LAMP reactions using a standard 96-well plate in a device the size of a lunchbox. This device features a novel optical arrangement to decrease power consumption, increase resolution, and eliminate cross-interference while analyzing 96 individual wells using three distinct excitation wavelengths. We will first discuss the mechanical features of the MINI device that make it highly accessible for POC use in limited-resource settings. We then elucidate the unique features of MINI that make it possible to analyze 96 samples simultaneously while only requiring a simple laptop-USB connection for power. We show the consistency of amplification and analysis in MINI by testing

positive and negative controls in completely full 96-well plates. Finally, we test MINI using two different LAMP assays and compare performance to a commercial qPCR device. To our knowledge, this is the first portable, high-throughput device capable of analyzing 96 independent samples using LAMP for POC diagnosis and screening.

3.3 Materials and Methods

3.3.1 MINI device – mechanical components and construction

Aluminum pieces were fabricated out of 6061-T aluminum by the Cornell Machine Shop. The aluminum outer case of MINI was designed in-house at Cornell and manufactured by ProtoCase. Temperature storage and stabilization is accomplished using a phase-change material specific to 65°C(OM65P-5X6-100, SavENRG), with 250 grams of material melted in a beaker and added to the outer basin of MINI. Heating via flame was performed using a portable butane burner (MTAMT-30, Master) while the MINI bottom panel was removed and the device elevated 4” using two aluminum blocks. Insulation within the device is lightweight melamine foam insulation sheets 1” thick (9249K24) obtained from McMaster-Carr and trimmed to fit with a knife. All minor hardware and fasteners were also sourced from McMaster-Carr. The optical filter within the device was custom ordered through Omega Optical as a 4” by 3” 530/660nm dual-bandpass filter.

3.3.2 MINI device – electrical components and construction

The three PCBs (Main, Top, Bottom) were designed using Autodesk – Eagle software and manufactured overseas at PCBWay. All the components were soldered in-house to supervise the electrical performance as the components were added. Two electrical

subsystems are controlled by a Teensy 3.6 microcontroller – optical and temperature. The optical subsystem comprises of two 8-bit shift registers (MM74HC595SJ), 24 RYB LEDs (SMTL4-SRYB), and 96 light to frequency converters (TSL237T) purchased from DigiKey. The temperature control subsystem has 3 temperature sensors (2 AD22103KRZ, 1 TMP512), 1 K-type thermocouple(Omega size #8 Screw size), and 1 cartridge heater (MCH1-240W-004, COMSTAT). All electrical components are powered via USB laptop connection with a micro-USB cable type B except the cartridge heater, which uses a separate 12V/6A power supply (SGA60U12-P1J).

3.3.3 Electrical operation of MINI

MINI temperature control and data acquisition is performed using an on-board microcontroller, while data storage and analysis is accomplished using a custom software capable of running on any standard laptop. The operation of the optical subsystem consists of cycling through the LED wavelengths while taking light measurements. The shift registers turn photodiode columns ON/OFF, enabling data acquisition with only eight analog pins. Before the final design, subsystems were tested separately using breadboards and off-the-shelf components. Temperature control is achieved through a custom algorithm using the four temperature measurements and the cartridge heater, ensuring component integrity during rapid heating.

3.3.4 Custom software – post-processing and threshold time calculation

The custom software was written using Python 3.7. After data acquisition, the software processes the curves by first running a Hampel filter (window = 11, standard dev. = 3)

followed by taking the first discrete difference of element (fluorescent difference). A second Hampel filter is then applied (window = 5, standard dev. = 1) to remove any random voltage drop along with a rolling mean (window = 10) to smooth the data. Reconstruction of the curve is then obtained through the cumulative sum. Threshold calculation is done by applying a threshold of 0.03 on the fluorescent difference curves and tracing this point back to its respective time. In the case where this threshold is not surpassed (no amplification), the threshold time is set to end of the run.

3.3.5 LAMP assay for KSHV

Six primers for target *Orf26* of KSHV[80] [Table B.1] synthesized by IDT were added to a mastermix consisting of isothermal amplification buffer, dNTP mix, $MgSO_4$, nuclease-free water, and Bst 2.0 WarmStart polymerase, all from New England Biolabs [Table B.2]. Each well of the 96-well plate (AB-0600, Thermo Scientific) received 35µL of mastermix and 5µL of DNA sample. Each sample well was topped with 50µL of laboratory-grade mineral oil to prevent evaporation during the run. Stocks of KSHV plasmid DNA samples were utilized from a previous publication[30] to create the positive and negative controls, as well as generate the standard curves for both MINI and the commercial device.

3.3.6 LAMP assay for GAPDH

Six primers for the housekeeping gene of GAPDH [Table B.3] were added to a mastermix of isothermal amplification buffer, $MgSO_4$, dNTP mix, Bst 2.0 WarmStart polymerase, and nuclease-free water (all from New England Biolabs). The exact

composition of the assay can be found in the supplemental information [Table B.4]. Each sample well of the 96-well plate received 45µL of mastermix and 5µL of DNA sample, after which each sample well was topped with 50µL of mineral oil to prevent evaporation during the run. GAPDH DNA samples were produced using the QIAGEN DNeasy Blood and Tissue kit (69504, QIAGEN) using tissue samples received from a collaborator at Weill Cornell Medicine. Overnight extraction was completed prior to the purification protocol from QIAGEN followed exactly per manufacturer's recommendations. Extracted DNA concentration was measured using a SpectraMax QuickDrop micro-volume spectrophotometer using 1.0µL of sample. GAPDH copy number was then estimated using the weight of the human genome[81] and dilutions were performed using the AE elution buffer from the QIAGEN DNeasy kit.

3.3.7 Isothermal amplification using the QuantStudio 7

The normal temperature-cycling profile was replaced with a single ramp from room temperature to 65°C, followed by 150 repeated holds at 65°C to enable a total assay time of 50 minutes with measurements taken every 20 seconds, closely mimicking the MINI device. Samples run on the QuantStudio 7 did not have mineral oil added as there is a heated top plate to prevent evaporation.

3.4 Results and Discussion

3.4.1 Instrument design and heating characteristics

MINI was developed to serve as a high-throughput point-of-care device for isothermal nucleic acid testing. The device is easily portable to various testing sites with dimensions around the size of a standard lunchbox – 12 inches long by 8 inches wide by 5 inches high – and weighing under 10 pounds fully assembled [Figure 3.1A]. Two nested rectangular basins – inner and outer – are used to hold the optical system and the phase change material (PCM), respectively [Figure 3.1B]. The design and construction utilizing two nested aluminum basins makes it possible to exchange the PCM with one that melts at a different temperature, providing flexibility for different assay requirements.

An inset cartridge heater in the outer basin is used to heat the device when electricity is available, and heat sinks added to the outer basin interior to allow for faster heat transfer into the PCM. The PCM within the MINI has a long thermal dwell at 65°C as it transitions from solid to liquid, storing heat energy as it melts completely in about 72 minutes [Figure 3.1C]. This enables MINI to continue to maintain temperature within 1°C for over 90 minutes in the event of electricity loss [Figure 3.1D]. There is only a slight 2.5°C temperature difference between wells in the center of the array and wells on the periphery after almost two hours of cooling. There is effectively no temperature difference between central and peripheral wells while electric power is present. Temperature uniformity across the 96 sample wells indicates that there should be no difference in amplification activity between samples. While heating by electricity was accomplished in just over 70 minutes, exchanging our current cartridge heater for a

higher-wattage equivalent could produce faster heating times.

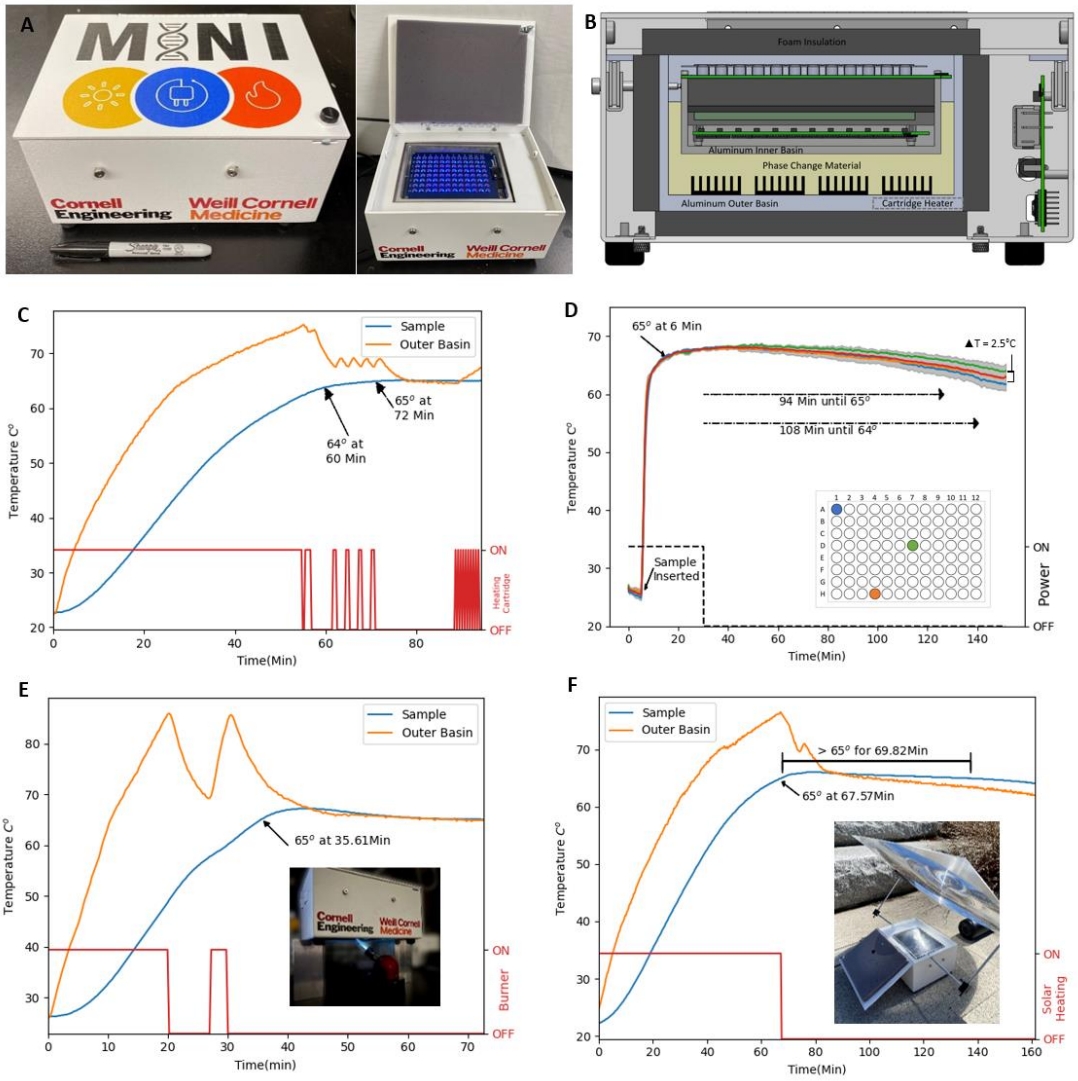

Figure 3.1 – MINI mechanical and heating properties. (A)MINI is 12 inches long by 8 inches wide by 5 inches high and weighs less than 10 lbs. (B) Cross-sectional view shows the two nested aluminum basins (inner and outer) with PCM between. Sample measurement system is contained within the inner basin. (C) Heating via electricity-powered cartridge heater takes ~72 minutes to reach the desired temperature of 65°C to fully melt the PCM. (D) A fully-loaded 96-well plate reaches reaction temperature within 6 minutes. In the event of electricity-loss, MINI maintains an average temperature of 65°C for over 90 minutes. At 108 minutes, there is a difference of 2.5°C between the central and corner sample wells. (E) Heating via flame is accomplished with 23 minutes of applied flame and stabilizes at reaction temperature in 36 minutes total. (F) Heating using a Fresnel lens ($4ft^2$) projected onto a black, aluminum top plate is accomplished in ~68 minutes.

MINI is also capable of heating using alternate energy sources when electricity is not present, such as flame or solar energy. The bottom of the device is removable, allowing a small butane burner to heat the device in ~33 minutes [Figure 3.1E]. For solar heating, an aluminum plate painted black is rested on the walls of the outer basin and a large Fresnel lens ($4ft^2$) was attached to focus solar rays in the center of the plate. Using this setup, we were able to fully melt the PCM in just over an hour on a sunny day in New York [Figure 3.1F]. The test began at 12:00 noon with an air temperature of 19°C and an intermittent 10-14kph breeze. However, even with successful solar heating, the large Fresnel lens does somewhat reduce the portability and simplicity of the device compared to a small flame source such as a butane-powered burner.

3.4.2 Optical and electrical design to enable 96 sample capacity

The optical system serves to illuminate the 96 sample wells and collect the resulting data, which can include fluorescence, colorimetric, or turbidity measurements. A top printed circuit board (PCB) holds 24 light emitting diodes (LEDs) that illuminate four adjacent sample wells, where light then continues out of the bottom of the sample, through an optical filter, and is collected by photodiodes on a second PCB below [Figure 3.2A]. This compact LED arrangement allows MINI to utilize readily available 96-well plates similar to commercially available machines.

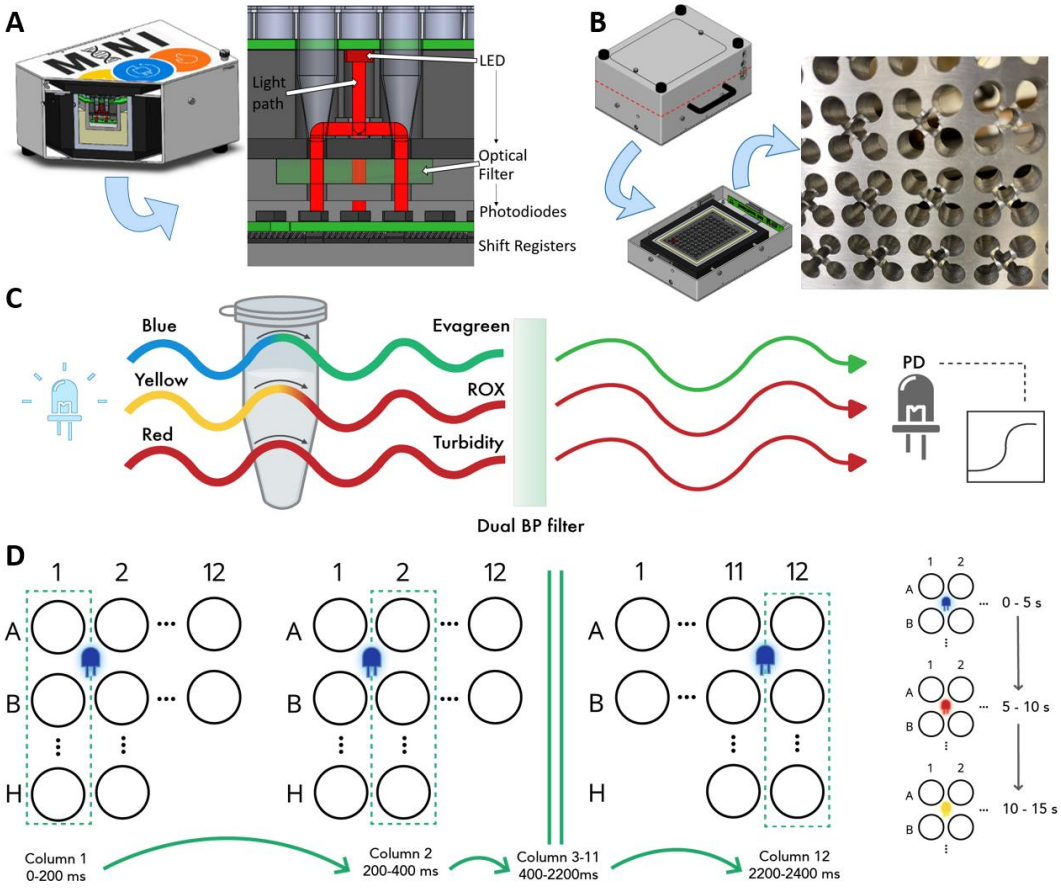

Figure 3.2 – MINI optical and electronic properties. (A) Light emitted from LEDs on the top PCB travels down and splits to illuminate four adjacent sample wells. Light continues out of the bottom of each sample well, through the optical filter, and is collected by photodiodes below. (B) Each sample well is connected to the LED using individual channels created with an end-mill. The channels are used to completely isolate each sample well from every adjacent sample well. (C) Different wavelengths of light are used to illuminate the samples and measure different emission spectra for fluorescence, normalization, and turbidity. (D) Each column is analyzed over 200ms, requiring 2.4 seconds to complete all 96 measurements for a single wavelength. Additional time added for LED stabilization and temperature measurements brings the total collection time for each wavelength to 5 seconds, and a total data collection cycle time of 15 seconds.

In order to optically isolate adjacent sample wells, as well as minimize the amount of electronics needed – using only 24 LEDs for 96 total samples – MINI utilizes a unique machined design. Individual channels were created within the aluminum sample block using an end-mill to allow light from each LED to illuminate the four adjacent sample wells [Figure 3.2B]. Each sample well is only connected to a specific LED, without any

connections to nearby LEDs or samples, so there is minimal optical noise between samples. Further noise reduction was achieved by increasing the light path length with a black plastic spacer beneath the milled aluminum piece, minimizing any reflected light from the shiny metal above. With this design, we are able to (1) fully isolate each sample from the influence of an adjacent well, and (2) minimize the electronic requirements of the device, allowing us to use only 24 LEDs for illumination. This arrangement also minimizes the overall size of the device, where LEDs are inset between the sample wells instead of above like in a traditional analyzer.

Each of the 24 LEDs cycles from blue to yellow to red, enabling measurement of multiple parameters [Figure 3.2C]. Blue light can be used to measure fluorescence of Evagreen dye, yellow light is used for a normalization dye such as ROX, and red light can be used to measure the turbidity of the reaction. The dual bandpass filter that MINI uses only allows green(530nm) and red(660nm) wavelengths to pass, further increasing the quality of our signal. Due to the large number of wells and limited number of analog inputs on the microcontroller, MINI employs two 8-bit shift registers that switch on a single column of wells at a time. Data for each column is collected over a 200ms span before moving to the next column [Figure 3.2D]. In total, 2400ms or 2.4 seconds are used to acquire data from all 96 wells for a single LED wavelength. Each measurement cycle also includes additional time to allow for LED stabilization and temperature recordings, bringing the total time to 5 seconds for each wavelength and 15 seconds for a complete data acquisition cycle. We also have the ability to expand the optical (LED and filter) components for other excitation and emission wavelengths, increasing the number of assays MINI can run.

After a successful run, MINI generates 288 light intensity curves (96 wells and 3 wavelengths) which are analyzed by custom Python software. Data processing consists of a series of Hampel filters to eliminate noise and correct for potential voltage drops. The software then determines the amplification threshold time (in minutes) or determines there was no amplification.

3.4.3 Determining performance of optical isolation design using positive and negative controls

In order to validate the novel optical isolation design and electronic circuitry across all 96 sample wells, we utilized a LAMP assay for Kaposi's sarcoma associated herpesvirus (KSHV). We ran two separate plates with 79 positive (PC) and 17 negative (NC) controls arranged to satisfy many possible testing combinations – one NC per row/column, differing number of adjacent PC, etc. [Figure 3.3]. Using positive control samples with expected strong amplification curves, we can analyze various levels of potential adjacent sample interference. Essentially, does a negative sample surrounded by positive samples still produce the expected negative result or is there influence from the surrounding strongly amplifying positive samples?

Overall standard deviation between PC threshold times was 50 seconds, showing consistent results across all 96 wells of the device. We saw strong amplification in all PC samples and no amplification in any NC samples, meaning adjacent sample wells are sufficiently isolated from each other. Additionally, we found no significant trend with sample location – peripheral, central, or corner sample wells – and threshold time, reinforcing our previous assessment of good temperature uniformity across the device.

This test was repeated in a mirrored fashion to ensure repeatability between runs despite different sample configurations. In both runs, we found a similar standard deviation between positive controls that did not correlate with position within the 96-well plate, as well as 100% accuracy of PC/NC amplification by the MINI and accompanying software.

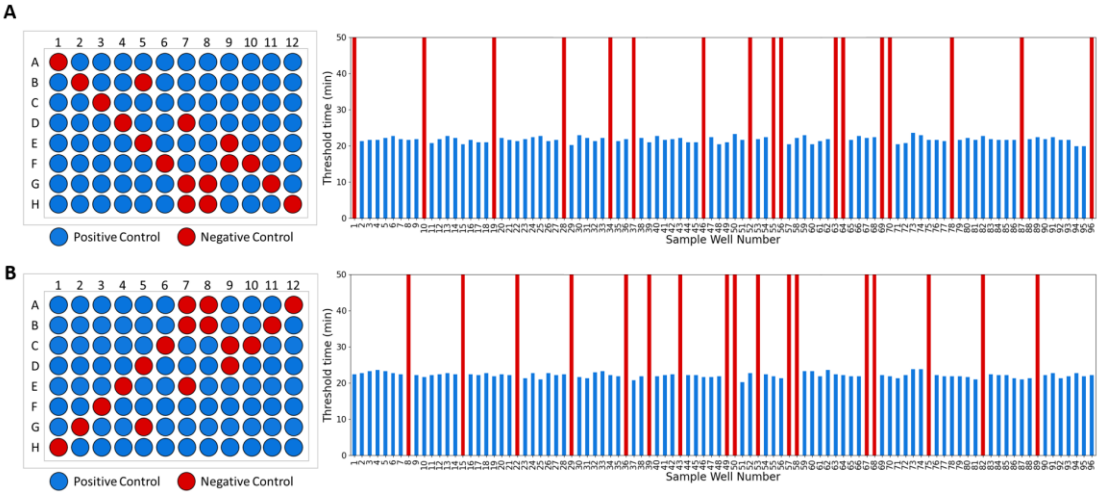

Figure 3.3 – MINI stability across 96 sample wells. Positive and negative controls for a KSHV LAMP assay were run in differing configurations (A and B) in the MINI to assess the performance of our unique optical design. Consistent positive control amplification, as well as consistent non-amplification of the negative controls, indicates that each sample well is fully isolated from all adjacent wells.

3.4.4 Comparison to a commercial analyzer using two LAMP assays

To further assess the performance of MINI, we tested serial dilutions using two different LAMP assays and compared performance to a QuantStudio7 commercial qPCR device[Figure 3.4]. The first LAMP assay utilized KSHV plasmid samples ranging from 300,000 copies per reaction down to 96 copies per reaction. These samples were tested in the same plate as a second LAMP assay using GAPDH genomic DNA samples ranging from ~120,000 copies per reaction to ~100 copies per reaction. Each dilution

was tested in triplicate for both assays used. Standard error increased at lower copy numbers of both DNA samples tested which is consistent with earlier use of these assays, and likely not due to any limitation of the MINI device as evident by the error increasing for the commercial device as well. Overall, the MINI produced comparable results to the commercially available analyzer, indicating that our unique configuration for 96 sample analysis maintains analytical performance.

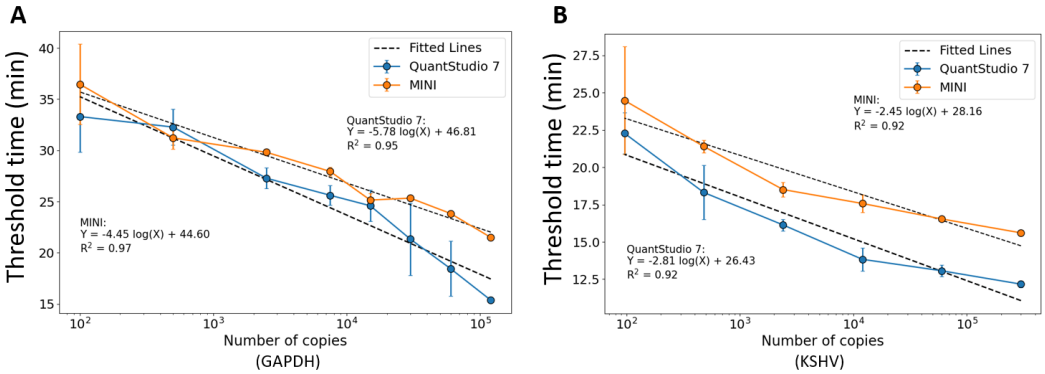

Figure 3.4 – MINI performance compared to commercial device. Standard curves were generated from serial dilutions analyzed in the MINI and a commercial amplification device, the QuantStudio 7. (A) GAPDH dilutions from ~120,000 copies per reaction down to ~100 copies per reaction show similar performance between the two devices, with MINI having overall smaller error between samples. (B) KSHV plasmids ranging in concentration from 300,000 copies per reaction to 96 copies per reaction showed very similar performance and overall low error.

3.4.5 A high-throughput, point-of-care device for limited-resource settings

There are a number of infectious diseases that could benefit from high-throughput molecular analysis, especially in developing nations. Cervical cancer through HPV infection, vector-borne diseases like malaria, and highly transmissible diseases like tuberculosis and SARS-COV-2 all have high disease burdens in limited-resource nations that could benefit from improved access to screening technologies. Nucleic acid

amplification technologies such a qPCR is commonly used for diagnosis of many infectious diseases, but is difficult to apply in limited resource settings[57]. Some success has been had with instruments like the GeneXpert by Cepheid for tuberculosis and Covid-19 testing, but this machine is still cost- and resource-demanding[49, 50]. Many isothermal amplification technologies are under development for point-of-care testing, which have very clear benefits for use in developing nations due to device and assay simplicity, reduced cost, and accessibility[57, 58]. However, there is a technological gap between current advances – capable of testing tens of samples per day – and the high-throughput testing – capable of hundreds of samples per day – needed to provide sufficient capacity for mass screening and point of care diagnosis.

In remote settings, decentralized approaches such as community screening programs can increase access to testing where hospitals and clinics require distant travel and high costs[55]. For cervical cancer screening through HPV testing, MINI offers the ability to multiplex assays and screen for multiple high-risk HPV strains. As an example, cervical swabs for eight women could be screened for 12 of the 14 HPV subtypes that are high-risk for cancer in a single run. For outbreaks of tuberculosis or malaria, and more recently COVID-19, the portable and energy-flexible MINI could offer a solution for testing large communities of people – potentially hundreds of tests in only a few hours – in non-standard settings such as schools or other public venues. Additionally, at a given reaction temperature, multiple assays can be performed within the same run due to the large number of sample wells, such as screening 48 patients for COVID-19 and tuberculosis simultaneously.

3.5 Conclusions

Our device MINI is the first POC accessible device capable of analyzing 96 samples per run. It is well-suited for point-of-care testing as it is easily portable and simple to operate, as well as capable of maintaining functionality without electricity, if necessary. We have developed a unique optical and electronic configuration to ensure complete isolation between samples while producing a compact POC device with limited complexity and number of electronics required. Validation was performed by testing all 96 wells simultaneously using differing arrangements of positive and negative controls. We have also shown MINI has comparable quantification performance to a commercial amplification device using two different LAMP assays for both KSHV and GAPDH. Future efforts will include increasing the flexibility of MINI to additional isothermal assays as well as deployment and testing in resource-limited settings. A point of care device such as MINI that can be used in decentralized healthcare settings at local clinics could provide more timely diagnoses and subsequent initiation of treatment, potentially improving health outcomes for these diseases.

3.6 Acknowledgements

We would like to acknowledge our extensive list of collaborators and colleagues that provided insights during development. Additional thanks to Cornell Machine Shop manufacturing help. This work was supported by the National Institutes of Health/National Cancer Institute through a supplement to grant UH2/UH3CA202723.

CHAPTER 4

RAPID NUCLEIC ACID EXTRACTION FROM TISSUE BIOPSIES USING A POINT-OF-CARE DEVICE***

4.1 Abstract

Nucleic acid extraction is often the rate-limiting step of many sample-processing protocols for diagnostic testing, especially for larger sample types such as tissue biopsies. Laboratory standard techniques often utilize lengthy enzymatic digestions to release DNA from tissue, reducing the impact of downstream point-of-care diagnostics. Recent advances for point-of-care extraction largely focus on pathogenic bacteria or viruses, and are ineffective for large, robust tissue samples. With increasing research into point-of-care molecular diagnosis of dermatological diseases using skin biopsies, there is a clear need for sample processing innovation. To address this, we have developed BLENDER, a device for rapid nucleic acid extraction from tissue biopsies that combines bead-beating homogenization with simultaneous sample heating for enzymatic lysis. Our device is able to produce a complete DNA yield from a 3mm cylindrical skin biopsy with only a 15-minute extraction compared to 4 hours when using a commercially available extraction protocol. Decreasing sample-processing time for tissue biopsies could decrease time-to-result for downstream analysis, enabling faster point-of-care diagnosis of solid cancers in limited resource settings.

***This work by Duncan McCloskey and David Erickson was accepted for publication in *Lab on a Chip* as of June 2022.

4.2 Introduction

Nucleic acid testing (NAT) is becoming increasingly important for disease diagnosis, especially in limited-resource settings. Point-of-care (POC) diagnostic approaches can provide increased access for patients where decentralized healthcare is common, as well as reduced time-to-result compared to traditional testing methods such as bacterial culture or pathology analysis [31, 33, 82]. There have been advancements towards nucleic acid diagnosis for a multitude of skin diseases, ranging from fungal or bacterial infections[29, 39, 41] to dermatological cancers like Kaposi's sarcoma[42]. However, sample processing is often the rate-limiting step towards timely NAT for any robust sample type such as skin tissue biopsies.

Prior to nucleic acid-based diagnosis, genomic, bacterial, or viral DNA is extracted from a patient sample, purified of extracellular debris and inhibitory compounds, and amplified with a technique such as the quantitative polymerase chain reaction (qPCR) or another similar assay. There are various methods available for the extraction of nucleic acids from tissue, most commonly using a combination of proteinase enzymes and heated incubation[83]. However, for tissue biopsies, this incubation step can require 4 hours or longer, which limits the POC potential of many NAT approaches due to the longer time-to-result. POC nucleic acid extraction technologies under development largely focus on pathogenic detection from liquid samples and commonly utilize droplet-based microfluidics with no carryover to large tissue extractions [84-87].

Homogenization is a mechanical lysis technique that can be used to fully disperse sample tissue and reduce digestion times for enzymatic extractions[88, 89].

Available laboratory techniques include grinding with a pestle and mortar[90, 91] (usually after flash-freezing with liquid nitrogen), or homogenization using a rotor stator device. However, these are not feasible for POC applications due to the equipment and safety requirements for use, including sterilization before/after each sample and open-air operation. Bead-beating is another homogenization technique that mechanically disperses the tissue sample through vigorous shaking of the tissue and a lysing bead, and has been shown to produce equivalent DNA to other homogenization techniques[92]. There are clear benefits for POC use, as bead-beating can be accomplished using inexpensive disposable tubes and beads, as well as being fully contained – meaning samples are safely within a closed tube during homogenization unlike alternative methods mentioned previously. However, commercially available bead-beating instruments are not suitable for POC use in limited resource settings due to high cost, power requirements, and lack of portability. Additionally, commercial bead-beaters – as well as other homogenization solutions – do not have the ability to keep samples at temperatures suitable for enzymatic digestion, requiring an additional heating device for complete DNA extraction. Innovations for POC bead-beating largely focus on pathogenic detection[93-95], such as an audio-powered bacterial lysis device used for tuberculosis[96]. However, none of these approaches is viable for larger samples, especially "tough" tissue types like skin that have increased amounts of connective proteins. A POC approach for rapid DNA extraction from skin was developed for the detection of *Leishmania* bacteria[97]. However, this approach requires manual disruption of the tissue sample during heated lysis using a toothpick, which can incur additional safety hazards during processing.

Here, we present the development of a device called BLENDER to perform Bead-beating Lysis with Enzymes for Nucleic aciD ExtRactions. BLENDER is a POC-accessible device for the homogenization and complete digestion of large tissue samples, such as skin biopsies, for downstream NAT and molecular analysis. Utilizing simultaneous bead-beating and enzymatic lysis methods, BLENDER is capable of rapid nucleic acid extraction from 3mm skin biopsies in only 15 minutes, whereas traditional enzyme-only digestions can take 4 hours or longer. We first discuss the mechanical features and construction of the device, as well as bead selection for skin tissue homogenization. We then demonstrate the effectiveness of BLENDER by producing complete DNA yields with a rapid 15-minute extraction, comparable to a 4-hour long extraction using a commercially available protocol. Finally, we test extracted DNA from both methods using qPCR and show equivalent amplification performance for downstream testing. Rapid sample processing could decrease the time-to-result for many NAT technologies and increase the impact of molecular diagnostics in limited resource settings.

4.3 Materials and Methods

4.3.1 BLENDER construction and characterization

BLENDER is a small, benchtop device for DNA extraction from tissue biopsies, coupling homogenization via bead-beating with simultaneous enzymatic digestion at 56-65°C [Figure 4.1A]. The device utilizes a 3D-printed ABS chamber with an acrylic front panel as the sample processing chamber, while the accompanying electronics and motor are kept in a separate chamber behind [Figure 4.1B]. The sample-processing chamber has a removable lid and front acrylic for easily inserting samples, yet completely sealing off the chamber while DNA extraction occurs [Figure 4.1C]. The processing chamber includes a tube holder attached to a Scotch yoke mechanism for homogenization, as well as a non-contact aluminum heat block for simultaneous enzymatic digestion of the tissue. The motor-driven Scotch yoke mechanism utilizes a 3D printed frame with inset linear bearings on both sides and an aluminum guide in the center [Figure 4.1D]. BLENDER utilizes a high-RPM motor with encoder for precise high- or low-RPM actuation of the Scotch yoke. The motor attaches to an aluminum wheel with a brass follower – this follower post is trapped within the aluminum guide of the sample motor, though it can spin freely and move laterally within the guide. As the motor spins, the Scotch yoke translates circular motion up to 3000RPM into linear motion up to 50Hz. Concurrent with physical lysis through homogenization, samples also undergo enzymatic lysis using the non-contact aluminum heat block at the bottom of the device [Figure 4.1E]. With a target range of 56-65°C for optimal enzyme activity, BLENDER reaches the minimum temperature of 56°C in only 1 minute 30 seconds and the maximum target temperature of 65°C in 3 minutes 30 seconds. With the heat block

at operational temperature, the sample tube can then be inserted. Once inserted and lowered to the bottom position, 56°C is reached in 2 minutes and 65°C is reached in just over 4 minutes.

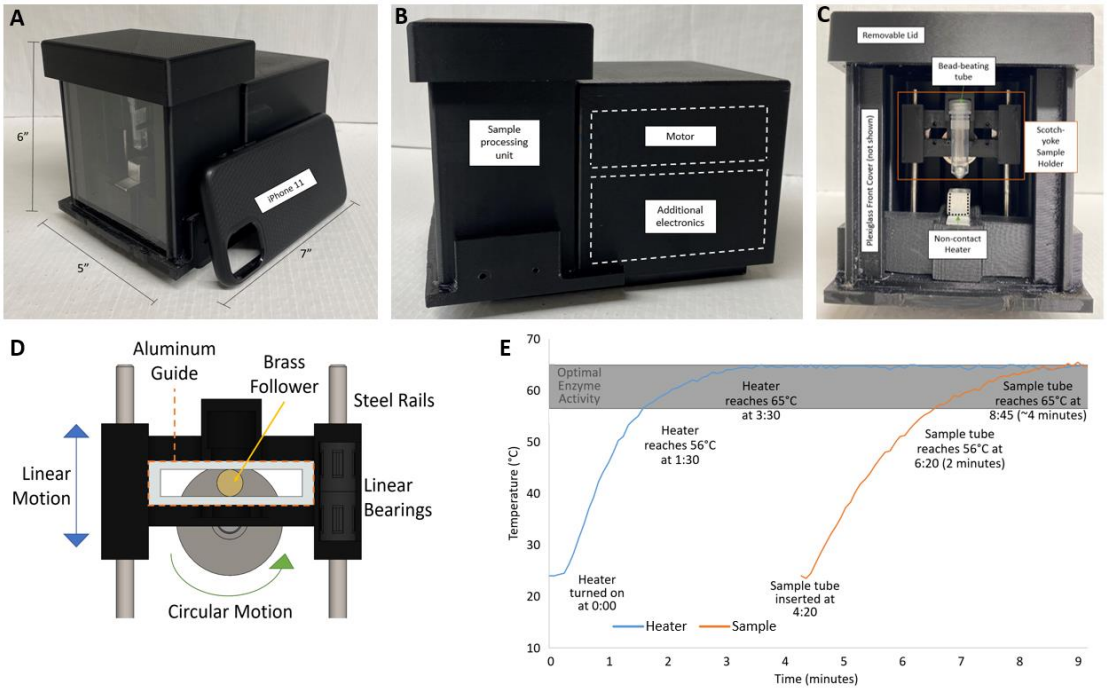

Figure 4.1 – BLENDER construction and operation. (A) BLENDER is a small, portable device for rapid DNA extraction from robust tissue biopsies for downstream diagnostic testing. (B) This device features two separate compartments: a front compartment for sample processing and a rear compartment to house the motor and other electronics. This makes it relatively simple to clean when necessary and protects the electronics while keeping them accessible. (C) The sample processing unit features a Scotch yoke tube holder and a non-contact aluminum heat block for simultaneous bead-beating and enzymatic digestion. This compartment also has a removable lid and acrylic front cover for easily inserting and monitoring samples while keeping any potential biohazards contained. (D) The sample holder is 3D printed using ABS and contains linear bearings for reduced-friction movement along the two linear rails. The motor-driven aluminum wheel of the Scotch yoke mechanism has a brass follower that is trapped within an aluminum guide attached to the 3D printed tube holder. As the motor-driven wheel spins, the Scotch yoke translates the circular motion into linear motion for sufficient bead-beating performance. (E) BLENDER uses simultaneous enzymatic digestion during the rapid DNA extraction, which requires temperatures between 56-65°C. From room temperature, the minimum target temperature is reached within 1.5 minutes and the maximum is reached 2 minutes later. Once the BLENDER is at temperature, an inserted sample will reach the minimum temperature of 56°C within 2 minutes and will reach the maximum target temperature of 65°C in just over 4 minutes.

4.3.2 Reagents and equipment

Standard lysis of skin biopsies was performed using the QIAGEN DNeasy Blood & Tissue kit (#69504, QIAGEN). Bead-beating required an additional anti-foaming Reagent DX (#19088, QIAGEN). Bead-beating was accomplished utilizing sterile 2ml screw-cap tubes and various homogenization inserts – garnet matrix (#11079110gar, BioSpec), zirconia beads (#11079124zx, BioSpec), small (#96415K68, McMaster-Carr) and large (#96415K75, McMaster-Carr) steel beads. Electronics used for homogenization include an Arduino Uno, a Pololu G2 simple motor controller (#1363, Pololu), and a ServoCity Yellowjacket 5201 motor (#5000-0002-4008, ServoCity). The motor was mounted using M3 fasteners and motor mounts from ServoCity. Electronics used for heating and temperature control include the above-mentioned Arduino Uno, two k-type thermocouples with accompanying MAX6675 temperature sensors (SainSmart), a 2" cartridge heater (#MCH1-240W-004, Comstat Inc.), and a 5V relay (#3-01-0340, HiLetGo). Operation of the BLENDER utilizes four 3/16" diameter linear bearings (#6489K71, McMaster-Carr) that move along two 4" long 3/16" diameter linear shaft (#1162K118, McMaster-Carr). Remaining components of the device were 3D printed in-house using a Lulzbot 2.0 printer and ABS filament.

4.3.3 Skin biopsy sample collection

A single, large piece of skin tissue (~15in^2) was provided by a collaborator at Weill Cornell Medical College in New York, NY. This singular sample tissue was used for all extraction experiments herein, in an attempt to keep DNA yields between biopsies as consistent as possible. The skin tissue was kept at -20°C except for when removing

additional biopsies for analysis. All biopsies used in this paper were taken using a standard 3mm punch biopsy tool and weighed immediately. Experiments were performed over multiple months, so ~8 biopsies were taken at a time to minimize potential freeze-thaw effects on the sample DNA.

4.3.4 DNA extraction using the DNeasy kit

DNA extraction was accomplished using the QIAGEN DNeasy Blood & Tissue kit. For non-homogenized samples, pre-weighed 3mm biopsies were added to a screw-cap tube. Lysis reagents from the QIAGEN kit were then added, including 180 µL of Buffer ATL and 20 µL of Proteinase K. For samples that would undergo bead-beating homogenization, a single 1/4" corrosion-resistant stainless steel bearing was inserted into the tube, and 10 µL of Reagent DX was added to prevent excessive foaming. For non-homogenized samples, tubes were added to a heat block kept at 56°C and vortexed every 30 minutes, per QIAGEN's recommendations.

4.3.5 DNA purification using the DNeasy kit

For all samples, extracted DNA was purified using the QIAGEN DNeasy Blood & Tissue kit. Lysate was allowed to cool to room temperature following enzymatic digestion. 200 µL of Buffer AL and 200 µL of 200-proof Ethanol were added to the lysate and mixed by vortexing before being pipetted into a DNeasy spin-column. Samples were centrifuged at 6,000xG for 1 minute to remove unwanted cellular debris. Spin columns were moved to a new collection tube and flow-through was discarded. 500 µL of Buffer AW1 wash buffer was added, samples were centrifuged for 6,000xG

for 1 minute, spin-columns were moved to a new collection tube, and flow-through was discarded. 500 µL of Buffer AW2 wash buffer was added, samples were centrifuged for 17,000xG for 3 minutes, spin-columns were moved to a sterile microcentrifuge tube, and flow-through was discarded. For the elution step, 75 µL of Buffer AE was added and let sit on the membrane for 1 minute. Samples were then centrifuged at 6,000xG for 1 minute to elute the purified DNA. Eluted DNA samples were stored at -20°C when not undergoing additional testing.

4.3.6 DNA analysis using spectrophotometer and qPCR

DNA analysis was done using a SpectraMax QuickDrop micro-volume spectrophotometer. The device was cleaned using DI water and blanked using Buffer AE as a reference. For each sample, 2.0 µL of sample was added, measured for DNA yield, and cleaned off using a Kimtech wipe. Each DNA sample was measured in triplicate using 3 separate 2.0 µL drops and the DNA concentration was averaged. Additional analysis was performed on some samples using the QuantStudio 7 commercial qPCR device. A *GAPDH* assay was performed with a total reaction volume of 10 µL, including: 5 µL of TaqMan Genotyping Master Mix (ThermoScientific, 4371355), 0.5 µL of a 20x GAPDH TaqMan Copy Number Assay (ThermoScientific, 4400292-Hs00483111_cn), and 4.5 µL of sample. All sample DNA analyzed with qPCR was diluted to a standard 9ng total DNA for each reaction. The reaction cycle proceeded with an initial hold at 50°C for 2 minutes, a hold at 95°C for 10 minutes, and then 40 cycles between 95°C for 15 seconds and 60°C for 60 seconds. All samples were run in duplicate against a standard plasmid curve.

4.4 Results and Discussion

4.4.1 Bead-beating optimization – insert and RPM selection

Bead-beating is a homogenization approach to fully disperse a tissue sample prior to enzymatic digestion. A bead or other insert is placed into a bead-beating tube containing lysis buffer and the tissue sample, which then undergoes vigorous shaking. The ideal protocol will produce a highly-dispersed sample throughout the lysis buffer, greatly increasing the surface area available to the digestion enzymes. There are two main factors to consider when developing a bead-beating approach: insert (bead) selection and RPM level/duration. Insert selection can vary depending on the sample type used, with a variety of commercially available options. For robust tissue samples such as skin biopsies, many of the beads used for bacterial lysis are completely ineffective and will just bounce off the tissue. When considering RPM speed and duration, too slow/short will produce little effect on the tissue, whereas too fast/long may eventually induce DNA damage and reduce the viability of downstream analysis.

We tried four different insert types that were suggested for large tissue pieces – small and large diameter steel bearings, cubic zirconia beads, and angular garnet pieces – at four different RPM speed/duration combinations [Figure 4.2]. At only 500 RPM, with a duration of 3 minutes, none of the inserts had very good performance and all of the skin biopsies were largely intact. Similar results were found at 1000 and 1500 RPM, where there were still large portions of tissue remaining. Both sizes of steel beads started to disperse the tissue, but were unable to reach complete homogenization. A final test of 3000 RPM was attempted for each insert type, with a reduced homogenization time of only 30 seconds to prevent unwanted DNA damage. Both sizes of steel bearings were

able to produce complete homogenization of the skin biopsies, indicated by the lack of large pieces remaining and consistent small particles throughout the lysis buffer. However, after testing multiple runs, the tubes containing small diameter bearings had a high incidence of breakage, where the large diameter bearings had no breakage in any runs. With comparable homogenization performance, the risk of breakage was too high with small diameter bearings and the single large diameter bearing was used moving forward.

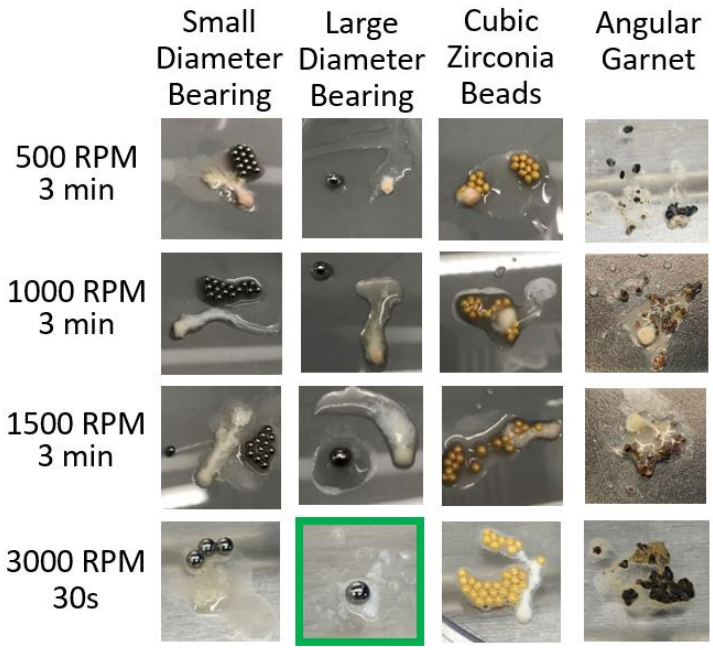

Figure 4.2 – Parameter optimization for homogenization of tissue biopsies. Various inserts – small and large diameter steel bearings, cubic zirconia beads, and angular garnet pieces – were tested for homogenization ability of skin tissue. Each insert type was tested using a range of RPM speed and duration from 500-1500 RPM for 3 minutes and 3000 RPM for 30 seconds. With the goal of a fully-dispersed tissue with no large intact pieces remaining, only the small and large diameter steel bearings at 3000 RPM were successful. All other combinations left biopsies largely intact, which would inhibit the rapid DNA extraction. Of the two possible choices, the singular large steel bead was selected due to a high incidence of tube-breakage when using the smaller diameter steel bearings.

With equal masses used for all bead selection trials, the cubic zirconia bearings seemed to lack the density to sufficiently penetrate and disperse the tissue biopsies. Angular garnet was indicated for skin tissue bead-beating by a commercial supplier; however, it did not seem to work well on the skin and instead just degraded the other pieces of garnet into a fine powder that coated the tissue. Steel beads were the clear choice for ideal skin biopsy homogenization, and the singular steel bead makes it very simple for future users – adding one bearing instead of counting or weighing multiple smaller ones. The only other consideration not shown here for bead selection was the switch to corrosion-resistant stainless steel beads, as some of the initial beads tested would start to visibly rust during the experiment.

4.4.2 DNA yields from standard and shortened extraction steps

With optimized insert, RPM level, and bead-beating duration, a complete tissue homogenization and DNA extraction was attempted using BLENDER. Three different DNA extraction methods were performed: (1) a control using the standard extraction protocol from QIAGEN with a 4-hour extraction time; (2) a shortened control using the same standard extraction protocol limited to only a 15-minute extraction time; and (3) a rapid DNA extraction using the BLENDER with a 15-minute total extraction time [Figure 4.3A]. Total sample processing time – the time required from start of patient visit to the time at which purified DNA is available for downstream NAT – includes the tissue biopsy removal and preparation, a DNA extraction step, and finally a DNA purification step.

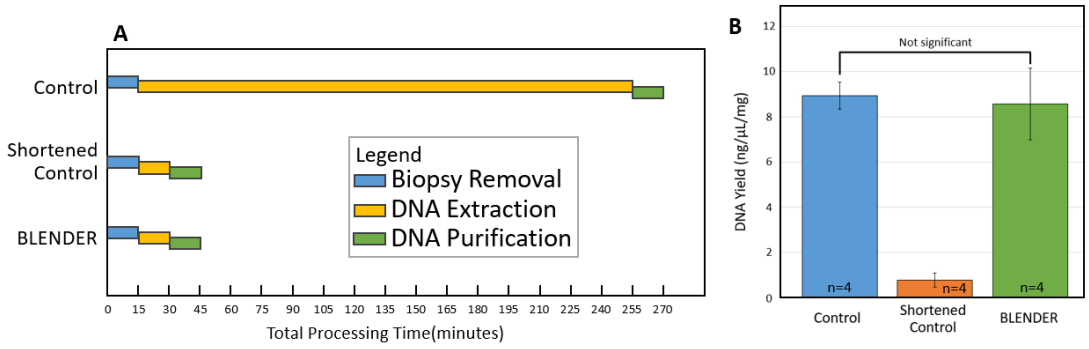

Figure 4.3 – Sample processing time and DNA yield comparison. (A) Total processing time, including biopsy removal, DNA extraction, and DNA purification, is shown for three separate protocols. The control protocol utilizes a standard commercial enzyme-only digestion with a 4-hour extraction time. The shortened control and BLENDER protocols were limited to a 15-minute extraction step. (B) BLENDER is capable of producing comparable DNA yields to the control protocol in a much shorter time. Whereas the shortened control that does not utilize homogenization produced very little DNA comparatively.

Quantifying the purified DNA yield from each of the three methods (n=4), we see no significant difference between the standard protocol control taking 4 hours and the BLENDER rapid extraction taking only 15 minutes [Figure 4.3B]. However, there is a very significant difference in the DNA yield when using a non-homogenized, shortened control with only a 15-minute digestion. This indicates that the complete homogenization and simultaneous enzymatic digestion can produce a complete DNA yield in only ~6% of the time of a standard digestion.

With many downstream NAT approaches requiring only 30-90 minutes for results, a 15-minute extraction step could enable same-day results rather than patients returning for a later follow-up. Additionally, 4-hour long extractions in this study were performed with an attentive operator, thoroughly mixing the sample by vortexing every 30 minutes throughout the extraction. In limited-resource settings, it may be difficult to demand as much attention from healthcare workers, meaning the extraction step would likely take even longer than 4 hours. A related approach produced amplifiable DNA

after a 10-minute digestion period with a manual homogenization step using a toothpick after 5 minutes[97]. However, this open-air homogenization increases safety risks when using hazardous samples in POC settings. Additionally, they utilized 2mm biopsies and note that there was still tissue remaining after the 10-minute cutoff, indicating an incomplete digestion of tissue. BLENDER is able to produce a completely clear lysate in 15 minutes using a 3mm skin biopsy within a completely contained system for maximum efficacy and safety in limited-resource settings.

4.4.3 DNA yield and amplification performance using qPCR

With equivalent performance between BLENDER's 15-minute extraction and a standard 4-hour control, the only remaining question of the viability of this approach is the downstream testing using the extracted DNA. Since the end goal of this approach is to produce DNA more quickly for later quantitative or qualitative testing, the DNA needs to be usable in common NAT modalities. A previous study suggested that bead-beating could reduce quantifiable DNA through excessive fragmentation that is not obvious in spectrophotometric measurements[98]. A qPCR assay for GAPDH, a housekeeping gene, was used to quantify the amplifiable DNA produced by each method to determine whether bead-beating homogenization would have a detrimental effect on DNA quality. The standard enzymatic digestion control was compared to a homogenized-tissue extraction (n=8), with comparable DNA yield between the two [Figure 4.4A]. Using a standard curve, GAPDH copy numbers for each sample was determined, with no significant different between the standard control extraction and the extraction using bead-beating [Figure 4.4B]. This indicates that the chosen bead-

beating parameters – single steel bead, 3000 RPM, 30 seconds – was optimal for fully dispersing the robust tissue while being gentle enough to keep the DNA viable for downstream amplification.

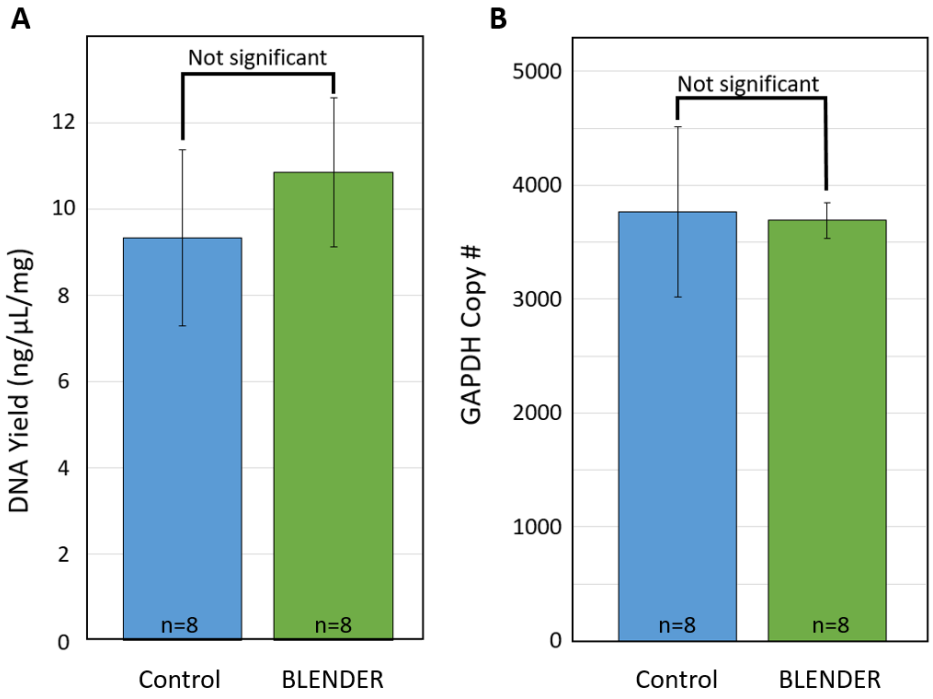

Figure 4.4 – DNA yield and qPCR amplification comparison. (A) The control protocol utilizing a 4-hour DNA extraction produces similar DNA yields to homogenized tissue. (B) A qPCR assay was performed to assess the viability of homogenized DNA for downstream amplification. GAPDH copy numbers were equivalent between both methods, indicating no detrimental effects of bead-beating to the extracted DNA.

4.5 Conclusions

Bead-beating homogenization using the BLENDER is a fully-contained, POC-accessible way to quickly disperse tissue within a lysis buffer. Simultaneous enzymatic digestion completely releases DNA as well as removes DNA-degrading extracellular proteins and qPCR inhibitors. Utilizing the BLENDER for a rapid DNA extraction, a complete DNA yield that is viable for downstream amplification can be produced in only 15 minutes compared to an average time of 4 hours using a standard commercial extraction protocol. Future improvements to the BLENDER can also be made to further increase the POC-potential, such as transitioning to battery power or even hand-crank actuation of the Scotch yoke. Greatly reducing the sample processing time required for downstream nucleic acid diagnostics could remove some of the barriers to rapid point of care diagnosis in limited-resource settings.

4.6 Acknowledgements

We would like to acknowledge our collaborators across the US and Africa for their insight and support. This work was supported by National Institutes of Health/National Cancer Institute grant UH2/UH3CA202723.

CHAPTER 5

CONCLUSIONS AND FUTURE DIRECTIONS

This dissertation detailed the development of three novel approaches for point-of-care nucleic acid-based diagnosis in an effort to increase access globally to rapid and accurate testing technologies. Chapter 2 detailed the development of a molecular approach to diagnose a dermatological cancer with very high prevalence and poor survivability in sub-Saharan Africa. Chapter 3 detailed an extension of that work by developing a device for testing greater numbers of patients per day, originally in an effort to address the COVID-19 pandemic and lack of testing available domestically, but with future applications in limited-resource settings. Chapter 4 detailed the development of a rapid nucleic acid extraction device that can quickly process larger tissue samples for downstream analysis.

Chapter 2 detailed a novel molecular approach for the diagnosis of Kaposi's sarcoma, which is one of the most common cancers in sub-Saharan Africa. Testing our approach on a cohort of 506 suspected-KS biopsies collected from patients at three clinics in Uganda, we were able to achieve 96% overall accuracy with high sensitivity and specificity. Compared to the current available methods for diagnosis – macroscopic examination or histopathology analysis – this molecular approach can offer a reduced time-to-result and increased accuracy in a point-of-care format. Future validation of this approach will be performed in "real-time" at several sites across Africa, where biopsy preparation, DNA extraction and purification, and LAMP-based analysis using the

TINY will all be performed locally. With continued success, this approach could be transformative to the diagnosis of Kaposi's sarcoma and improve outcomes for patients. By reducing the burden on limited healthcare infrastructure across sub-Saharan Africa and increasing access to timely diagnosis, earlier KS diagnosis could lead to faster application of therapy and result in improved survivability of this disease.

Chapter 3 detailed the development of a device for high-throughput nucleic acid testing as a solution for testing hundreds of patients per day at the point-of-care. The novel design of MINI was successful in providing complete optical isolation between all samples while maintaining a small device footprint capable of utilizing standard 96 well plates with minimal electronics. We showed even temperature profiles across the device and subsequent consistent amplification of positive controls, without any increased noise on adjacent negative samples. MINI also showed comparable performance to a commercial qPCR device, but with added benefits like solar heating, robustness against electrical power loss, and a rugged, portable packaging. The device itself can be improved further, with new photodiodes that would eliminate the need for a costly optical filter and increase the measurement capability of the device. For alternate assays, the PCM can be easily swapped for one that operates at a different temperature. Faster electrical heating could be accomplished by utilizing a higher wattage cartridge heater and further optimizing the heating parameters and basin design. Future applications of this device could include diagnostic testing for infectious diseases in limited-resource settings, such as tuberculosis testing in India and southern Asia or cervical cancer screening through HPV testing across sub-Saharan Africa.

Chapter 4 detailed the development of a novel device for rapid extraction of

nucleic acids from tissue biopsies for downstream analysis. BLENDER was capable of complete DNA extraction from 3mm biopsies in only 15 minutes, compared to 4 hours or longer using a standard commercially available method. Additionally, despite some previous publications questioning the effects of bead-beating on downstream DNA analysis, BLENDER-produced DNA had equivalent amplification performance to DNA produced by the commercial solid-phase extraction kit. Since the device is constructed using 3D-printed parts and inexpensive electronics, it should be accessible for point-of-care use alongside the TINY in local clinics across Africa. Combining the two technologies could reduce the overall time-to-result to under two hours post-biopsy removal, which would be transformative to the diagnosis of this cancer. Improvements to the device could include hand-powered actuation of the Scotch yoke using a reversed worm-gear mechanism for electricity-free bead-beating. Similarly, the aluminum within the device that functions for heat-transfer to the samples could be re-designed to allow alternate heating such as using a small butane Bunsen burner, again for electricity-free operation. However, since many of the clinics have some amount of electricity available, BLENDER could also just utilize a small battery to power the device for robustness against unstable electrical supply. Future efforts could also include a direct-to-LAMP approach where extracted DNA is used directly in the LAMP assay, rather than going through a roughly 15-minute purification process first. As a tandem device with the TINY, BLENDER could truly emphasize the impact of our diagnostic approach, offering a rapid and accurate diagnosis of a dermatological cancer in under two hours at the point-of-care.

APPENDIX A

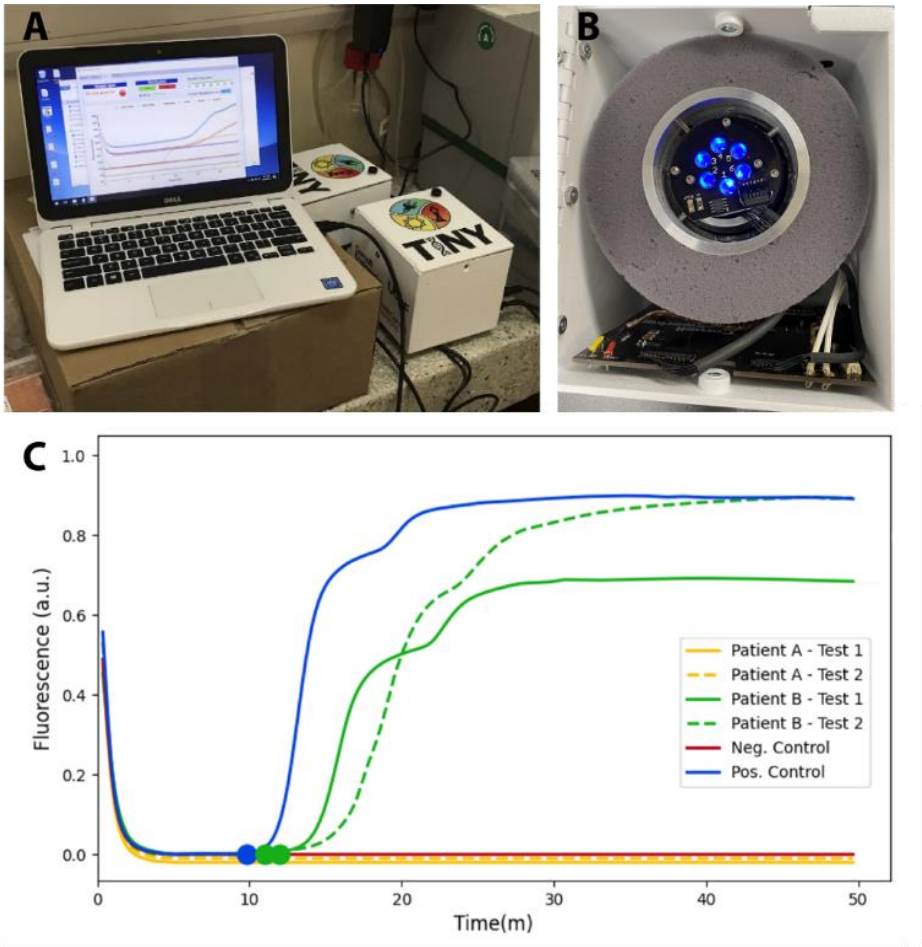

Figure A.1 – TINY device and LAMP example amplification curves (A) TINY being run off a ChromeBook in Uganda. (B) TINY internal view fully assembled. (C) An example test run using TINY shows the results for all six wells of the device. Two wells are used for positive (blue) and negative (red) controls. Patient A (green) and Patient B (yellow) were each tested in duplicate, with the solid line representing test 1 and the dashed line representing test 2. The large markers for positive control and Patient B represent where the threshold time is determined. Patient A results are shifted slightly below zero for visualization purposes.

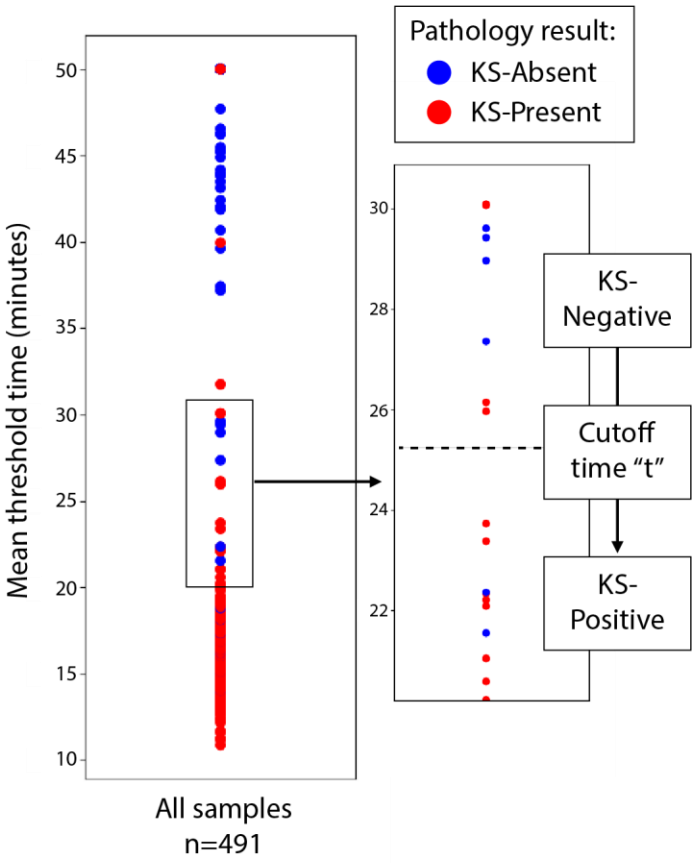

Figure A.2 – Thresholding for sensitivity and specificity generation. Cutoff time "*t*" is used to generate sensitivity and specificity of the KS-LAMP assay. At a given cutoff, samples that amplify before time "t" are considered positive for KS, and samples that do not are considered negative for KS.

APPENDIX B

Table B.1 – Primer sequences for KSHV-LAMP

Primer	**Sequence (5' > 3')**
F3	TGCCCCCTTTTTTCAGTGG
B3	CCGGCCGATATTTTGGAGT
FIP (F1c-F2)	TGGATTCGAGCACAATGGTGGACAACACCCAGCTAGCAGTG
BIP (B1c-B2)	TCGTGTTCCCCATGGTCGTGAGATGTGGTACACCAACAGC
LF	CCTTTCGGCTAAAAAATGGGGGTAG
LB	CAGCAACTGGGGCACGCTAT

Table B.2 – Mastermix composition for KSHV-LAMP

Reagent	**1X (µL)**
10X Isothermal Buffer	4.0
$MgSO_4$ (100 mM)	2.4
dNTPs (10 mM)	5.6
25X Primer Mix	0.88
Bst 2.0 WarmStart polymerase	1.6
8X Evagreen	2.0
5X ROX	1.6
Nuclease-free water	16.92
DNA Sample	5.0
Total	**40.0**

Table B.3 – Primer sequences for GAPDH-LAMP

Primer	**Sequence (5' > 3')**
F3	TGGGGAATGGGACTGAGG
B3	GTGGCAGTGATGGCATGG
FIP (F1c-F2)	TGGGAAAGCCAGTCCCCAGAA-CTCATCCAAGACTGGCTCCT
BIP (B1c-B2)	CTTTCAAGGTGGGGAGGGAGG- ACTGTGGTCTGCAAAAGGAG
LF	AACCCCAGGGTTGCACG
LB	TAGAGGGGTGATGTGGGGAGTA

Table B.4 – Mastermix composition for GAPDH-LAMP

Reagent	**1X (µL)**
10X Isothermal Buffer	5.0
$MgSO_4$ (100 mM)	3.0
dNTPs (10 mM)	7.0
25X Primer Mix	2.0
Bst 2.0 WarmStart polymerase	2.0
8X Evagreen	5.0
Nuclease-free water	21.0
DNA Sample	5.0
Total	**50.0**

REFERENCES

1. E. A. Mesri, E. Cesarman, C. Boshoff, Kaposi's sarcoma and its associated herpesvirus. *Nat. Rev. Cancer* **10**, 707-719 (2010).

2. Y. Chang, E. Cesarman, M. S. Pessin, F. Lee, J. Culpepper, D. M. Knowles, P. S. Moore, Identification of herpesvirus-like DNA sequences in AIDS-associated Kaposi's sarcoma. *Science* **266**, 1865-1869 (1994).

3. J. J. Russo, R. A. Bohenzky, M.-C. Chien, J. Chen, M. Yan, D. Maddalena, J. P. Parry, D. Peruzzi, I. S. Edelman, Y. Chang, Nucleotide sequence of the Kaposi sarcoma-associated herpesvirus (HHV8). *Proceedings of the National Academy of Sciences* **93**, 14862-14867 (1996).

4. D. H. Kedes, E. Operskalski, M. Busch, R. Kohn, J. Flood, D. Ganem, The seroepidemiology of human herpesvirus 8 (Kaposi's sarcoma–associated herpesvirus): distribution of infection in KS risk groups and evidence for sexual transmission. *Nature medicine* **2**, 918-924 (1996).

5. H. Sung, J. Ferlay, R. L. Siegel, M. Laversanne, I. Soerjomataram, A. Jemal, F. Bray, Global cancer statistics 2020: GLOBOCAN estimates of incidence and mortality worldwide for 36 cancers in 185 countries. *CA: a cancer journal for clinicians* **71**, 209-249 (2021).

6. D. E. McMahon, T. Maurer, E. E. Freeman, 25 years of Kaposi sarcoma herpesvirus: discoveries, disparities, and diagnostics. *JCO global oncology* **6**, (2020).

7. S. E. Krown, C. B. Moser, P. MacPhail, R. M. Matining, C. Godfrey, S. R. Caruso, M. C. Hosseinipour, W. Samaneka, M. Nyirenda, N. W. Busakhala, F. M. Okuku, J. Kosgei, B. Hoagland, N. Mwelase, V. O. Oliver, H. Burger, R. Mngqibisa, M. Nokta, T. B. Campbell, M. Z. Borok, Treatment of advanced AIDS-associated Kaposi sarcoma in resource-limited settings: a three-arm, open-label, randomised, non-inferiority trial. *The Lancet* **395**, 1195-1207 (2020).

8. M. Maskew, M. P. Fox, G. van Cutsem, K. Chu, P. MacPhail, A. Boulle, M. Egger, f. I. S. Africa, Treatment response and mortality among patients starting antiretroviral therapy with and without Kaposi sarcoma: a cohort study. *PloS one* **8**, e64392 (2013).

9. S. D. Makombe, A. D. Harries, J. K.-L. Yu, M. Hochgesang, E. Mhango, R. Weigel, O. Pasulani, M. Fitzgerald, E. J. Schouten, E. Libamba, Outcomes of patients with Kaposi's sarcoma who start antiretroviral therapy under routine programme conditions in Malawi. *Tropical doctor* **38**, 5-7 (2008).

10. A. Mosam, F. Shaik, T. S. Uldrick, T. Esterhuizen, G. H. Friedland, D. T. Scadden, J. Aboobaker, H. M. Coovadia, A randomized controlled trial of highly active antiretroviral therapy versus highly active antiretroviral therapy and chemotherapy in therapy-naive patients with HIV-associated Kaposi sarcoma in South Africa. *JAIDS Journal of Acquired Immune Deficiency Syndromes* **60**, 150-157 (2012).

11. P. Agaba, H. Sule, R. Ojoh, Z. Hassan, L. Apena, M. Mu'Azu, B. Badung, O. Agbaji, J. Idoko, P. Kanki, Presentation and survival of patients with AIDS-related Kaposi's sarcoma in Jos, Nigeria. *International journal of STD & AIDS* **20**, 410-413 (2009).

12. E. B. El Amari, L. Toutous-Trellu, A. Gayet-Ageron, M. Baumann, G. Cathomas, I. Steffen, P. Erb, N. J. Mueller, H. Furrer, M. Cavassini, Predicting the evolution of Kaposi sarcoma, in the highly active antiretroviral therapy era. *Aids* **22**, 1019-1028 (2008).

13. G. Nasti, F. Martellotta, M. Berretta, M. Mena, M. Fasan, G. Di Perri, R. Talamini, G. Pagano, M. Montroni, R. Cinelli, Impact of highly active antiretroviral therapy on the presenting features and outcome of patients with Acquired Immunodeficiency Syndrome–Related Kaposi sarcoma. *Cancer* **98**, 2440-2446 (2003).

14. F. Okuku, E. M. Krantz, J. Kafeero, M. R. Kamya, J. Orem, C. Casper, W. Phipps, Evaluation of a predictive staging model for HIV-associated Kaposi sarcoma in Uganda. *Journal of acquired immune deficiency syndromes (1999)* **74**, 548 (2017).

15. E. E. Freeman, A. Semeere, D. E. McMahon, H. Byakwaga, M. Laker-Oketta, S. Regan, M. Wenger, C. Kasozi, M. Semakadde, M. Bwana, Beyond T Staging in the" Treat All" Era: Severity and Heterogeneity of Kaposi's Sarcoma in East Africa. *Journal of acquired immune deficiency syndromes (1999)*, (2021).

16. E. B. El Amari, L. Toutous-Trellu, A. Gayet-Ageron, M. Baumann, G. Cathomas, I. Steffen, P. Erb, N. J. Mueller, H. Furrer, M. Cavassini, P. Vernazza, H. H. Hirsch, E. Bernasconi, B. Hirschel, Predicting the evolution of Kaposi sarcoma, in the highly active antiretroviral therapy era. *AIDS* **22**, 1019-1028 (2008).

17. G. Nasti, F. Martellotta, M. Berretta, M. Mena, M. Fasan, G. Di Perri, R. Talamini, G. Pagano, M. Montroni, R. Cinelli, E. Vaccher, A. D'Arminio Monforte, U. Tirelli, Impact of highly active antiretroviral therapy on the presenting features and outcome of patients with acquired immunodeficiency syndrome-related Kaposi sarcoma. *Cancer* **98**, 2440-2446 (2003).

18. K. M. Chu, G. Mahlangeni, S. Swannet, N. P. Ford, A. Boulle, G. Van Cutsem, AIDS-associated Kaposi's sarcoma is linked to advanced disease and high mortality in a primary care HIV programme in South Africa. *J Int AIDS Soc* **13**, 23 (2010).

19. K. Chu, G. Mahlangeni, S. Swannet, N. Ford, D. Stead, A. Boulle, G. Van Cutsem, paper presented at the 16th Conference on Retroviruses and Opportunistic Infections, Palais de Congres de Montreal, Montreal, Canada, February 8-11, 2009 2009.

20. E. Amerson, N. Buziba, H. Wabinga, M. Wenger, M. Bwana, W. Muyindike, C. Kyakwera, M. Laker, E. Mbidde, C. Yiannoutsos, Diagnosing Kaposi's Sarcoma (KS) in East Africa: how accurate are clinicians and pathologists? *Infectious Agents and Cancer* **7**, 1-2 (2012).

21. E. Amerson, C. M. Woodruff, A. Forrestel, M. Wenger, T. McCalmont, P. LeBoit, T. Maurer, M. Laker-Oketta, W. Muyindike, M. Bwana, Accuracy of clinical suspicion and pathologic diagnosis of Kaposi sarcoma in East Africa. *Journal of acquired immune deficiency syndromes (1999)* **71**, 295 (2016).

22. A. Adesina, D. Chumba, A. M. Nelson, J. Orem, D. J. Roberts, H. Wabinga, M. Wilson, T. R. Rebbeck, Improvement of pathology in sub-Saharan Africa. *The lancet oncology* **14**, e152-e157 (2013).

23. E. Amerson, A. Forrestel, L. Butler, M. Laker-Oketta, M. Bwana, T. Maurer, J. Martin, in *14th International Conference on Malignancies in AIDS and Other Acquired Immunodeficiencies*. (Bethesda, Maryland, 2013).

24. E. Cesarman, B. Damania, S. E. Krown, J. Martin, M. Bower, D. Whitby, Kaposi sarcoma. *Nature reviews Disease primers* **5**, 1-21 (2019).

25. C. C. Boehme, M. P. Nicol, P. Nabeta, J. S. Michael, E. Gotuzzo, R. Tahirli, M. T. Gler, R. Blakemore, W. Worodria, C. Gray, Feasibility, diagnostic accuracy, and effectiveness of decentralised use of the Xpert MTB/RIF test for diagnosis of tuberculosis and multidrug resistance: a multicentre implementation study. *The lancet* **377**, 1495-1505 (2011).

26. H. S. Cox, J. F. Daniels, O. Muller, M. P. Nicol, V. Cox, G. van Cutsem, S. Moyo, V. De Azevedo, J. Hughes, in *Open forum infectious diseases*. (Oxford University Press, 2015), vol. 2, pp. ofv014.

27. M. P. Nicol, L. Workman, W. Isaacs, J. Munro, F. Black, B. Eley, C. C. Boehme, W. Zemanay, H. J. Zar, Accuracy of the Xpert MTB/RIF test for the diagnosis of pulmonary tuberculosis in children admitted to hospital in Cape Town, South Africa: a descriptive study. *The Lancet infectious diseases* **11**, 819-824 (2011).

28. G. Theron, L. Zijenah, D. Chanda, P. Clowes, A. Rachow, M. Lesosky, W. Bara, S. Mungofa, M. Pai, M. Hoelscher, Feasibility, accuracy, and clinical effect of point-of-care Xpert MTB/RIF testing for tuberculosis in primary-care settings in Africa: a multicentre, randomised, controlled trial. *The Lancet* **383**, 424-435 (2014).

29. K. K. Sra, G. Torres, P. Rady, T. K. Hughes, D. A. Payne, S. K. Tyring, Molecular diagnosis of infectious diseases in dermatology. *Journal of the American Academy of Dermatology* **53**, 749-765 (2005).

30. R. Snodgrass, A. Gardner, A. Semeere, V. L. Kopparthy, J. Duru, T. Maurer, J. Martin, E. Cesarman, D. Erickson, A portable device for nucleic acid quantification powered by sunlight, a flame or electricity. *Nature biomedical engineering* **2**, 657-665 (2018).

31. P. Yager, G. J. Domingo, J. Gerdes, Point-of-care diagnostics for global health. *Annu. Rev. Biomed. Eng.* **10**, 107-144 (2008).

32. I. V. Jani, How point-of-care testing could drive innovation in global health. *The New England journal of medicine* **368**, 2319 (2013).

33. M. Urdea, L. A. Penny, S. S. Olmsted, M. Y. Giovanni, P. Kaspar, A. Shepherd, P. Wilson, C. A. Dahl, S. Buchsbaum, G. Moeller, Requirements for high impact diagnostics in the developing world. *Nature* **444**, 73-79 (2006).

34. J. Min, L. K. Chin, J. Oh, C. Landeros, C. Vinegoni, J. Lee, S. J. Lee, J. Y. Park, A.-Q. Liu, C. M. Castro, CytoPAN—Portable cellular analyses for rapid point-of-care cancer diagnosis. *Science Translational Medicine* **12**, (2020).

35. A. K. Mattox, C. Bettegowda, S. Zhou, N. Papadopoulos, K. W. Kinzler, B. Vogelstein, Applications of liquid biopsies for cancer. *Science translational medicine* **11**, (2019).

36. J. D. Cohen, A. A. Javed, C. Thoburn, F. Wong, J. Tie, P. Gibbs, C. M. Schmidt, M. T. Yip-Schneider, P. J. Allen, M. Schattner, Combined circulating tumor DNA and protein biomarker-based liquid biopsy for the earlier detection of pancreatic cancers. *Proceedings of the National Academy of Sciences* **114**, 10202-10207 (2017).

37. E. C. Oriero, J. Okebe, J. Jacobs, D. Nwakanma, U. D'Alessandro, Diagnostic performance of a novel loop-mediated isothermal amplification (LAMP) assay targeting the apicoplast genome for malaria diagnosis in a field setting in sub-Saharan Africa. *Malaria journal* **14**, 1-6 (2015).

38. J. Reboud, G. Xu, A. Garrett, M. Adriko, Z. Yang, E. M. Tukahebwa, C. Rowell, J. M. Cooper, based microfluidics for DNA diagnostics of malaria in low resource underserved rural communities. *Proceedings of the National Academy of Sciences* **116**, 4834-4842 (2019).

39. D. A. Payne, M. Vander Straten, D. Carrasco, S. K. Tyring, Molecular diagnosis of skin-associated infectious agents. *Archives of dermatology* **137**, 1497-1502 (2001).

40. B. L. Swick, in *Seminars in cutaneous Medicine and Surgery*. (WB Saunders, 2012), vol. 31, pp. 241-246.

41. G. W. Procop, Molecular diagnostics for the detection and characterization of microbial pathogens. *Clinical Infectious Diseases* **45**, S99-S111 (2007).

42. D. E. McMahon, L. Oyesiku, A. Semeere, D. Kang, E. E. Freeman, Novel Diagnostics for Kaposi Sarcoma and Other Skin Diseases in Resource-Limited Settings. *Dermatologic clinics* **39**, 83-90 (2021).

43. M. C. Pierce, D. J. Javier, R. Richards-Kortum, Optical contrast agents and imaging systems for detection and diagnosis of cancer. *International journal of cancer* **123**, 1979-1990 (2008).

44. J. M. Bland, D. Altman, Statistical methods for assessing agreement between two methods of clinical measurement. *The lancet* **327**, 307-310 (1986).

45. Coronavirus disease (COVID-19). (Geneva: World Health Organization), vol. 2022.

46. M. Jiang, W. Pan, A. Arasthfer, W. Fang, L. Ling, H. Fang, F. Daneshnia, J. Yu, W. Liao, H. Pei, Development and validation of a rapid, single-step reverse transcriptase loop-mediated isothermal amplification (RT-LAMP) system potentially to be used for reliable and high-throughput screening of COVID-19. *Frontiers in cellular and infection microbiology* **10**, 331 (2020).

47. T. M. Oeschger, D. S. McCloskey, R. M. Buchmann, A. M. Choubal, J. M. Boza, S. Mehta, D. Erickson, Early Warning Diagnostics for Emerging Infectious Diseases in Developing into Late-Stage Pandemics. *Accounts of Chemical Research* **54**, 3656-3666 (2021).

48. "Global tuberculosis report 2021." Geneva: World Heath Organization. 2021.

49. J. Chakaya, M. Khan, F. Ntoumi, E. Aklillu, R. Fatima, P. Mwaba, N. Kapata, S. Mfinanga, S. E. Hasnain, P. D. Katoto, Global Tuberculosis Report 2020–Reflections on the Global TB burden, treatment and prevention efforts. *International Journal of Infectious Diseases* **113**, S7-S12 (2021).

50. L. M. Parsons, Á. Somosközi, C. Gutierrez, E. Lee, C. Paramasivan, A. l. Abimiku, S. Spector, G. Roscigno, J. Nkengasong, Laboratory diagnosis of tuberculosis in resource-poor countries: challenges and opportunities. *Clinical microbiology reviews* **24**, 314-350 (2011).

51. D. Y. Wu, L. Ugozzoli, B. K. Pal, R. B. Wallace, Allele-specific enzymatic amplification of beta-globin genomic DNA for diagnosis of sickle cell anemia. *Proceedings of the National Academy of Sciences* **86**, 2757-2760 (1989).

52. L. Detemmerman, S. Olivier, V. Bours, F. Boemer, Innovative PCR without DNA extraction for African sickle cell disease diagnosis. *Hematology* **23**, 181-186 (2018).

53. F. Tekola-Ayele, C. N. Rotimi, Translational genomics in low-and middle-income countries: opportunities and challenges. *Public health genomics* **18**, 242-247 (2015).

54. C. Nakisige, J. Trawin, S. Mitchell-Foster, B. A. Payne, A. Rawat, N. Mithani, C. Amuge, H. Pedersen, J. Orem, L. Smith, Integrated cervical cancer screening in Mayuge District Uganda (ASPIRE Mayuge): a pragmatic sequential cluster randomized trial protocol. *BMC public health* **20**, 1-13 (2020).

55. M. Nakalembe, P. Makanga, A. Kambugu, M. Laker-Oketta, M. J. Huchko, J. Martin, A public health approach to cervical cancer screening in Africa through community-based self-administered HPV testing and mobile treatment provision. *Cancer medicine* **9**, 8701-8712 (2020).

56. N. T. Q. Nhu, D. Heemskerk, D. D. A. Thu, T. T. H. Chau, N. T. H. Mai, H. D. T. Nghia, P. P. Loc, D. T. M. Ha, L. Merson, T. T. V. Thinh, Evaluation of GeneXpert MTB/RIF for diagnosis of tuberculous meningitis. *Journal of clinical microbiology* **52**, 226-233 (2014).

57. G. A. Obande, K. K. B. Singh, Current and future perspectives on isothermal nucleic acid amplification technologies for diagnosing infections. *Infection and drug resistance* **13**, 455 (2020).

58. P. K. Drain, E. P. Hyle, F. Noubary, K. A. Freedberg, D. Wilson, W. R. Bishai, W. Rodriguez, I. V. Bassett, Diagnostic point-of-care tests in resource-limited settings. *The Lancet infectious diseases* **14**, 239-249 (2014).

59. T. R. Kozel, A. R. Burnham-Marusich, Point-of-care testing for infectious diseases: past, present, and future. *Journal of clinical microbiology* **55**, 2313-2320 (2017).

60. H. Zhang, Y. Xu, Z. Fohlerova, H. Chang, C. Iliescu, P. Neuzil, LAMP-on-a-chip: Revising microfluidic platforms for loop-mediated DNA amplification. *TrAC Trends in Analytical Chemistry* **113**, 44-53 (2019).

61. Z. Wei, X. Wang, H. Feng, F. Ji, D. Bai, X. Dong, W. Huang, Isothermal nucleic acid amplification technology for rapid detection of virus. *Critical Reviews in Biotechnology*, 1-18 (2022).

62. P. Craw, W. Balachandran, Isothermal nucleic acid amplification technologies for point-of-care diagnostics: a critical review. *Lab on a Chip* **12**, 2469-2486 (2012).

63. U. Morris, M. Khamis, B. Aydin-Schmidt, A. K. Abass, M. I. Msellem, M. H. Nassor, I. J. González, A. Mårtensson, A. S. Ali, A. Björkman, Field deployment of loop-mediated isothermal amplification for centralized mass-screening of asymptomatic malaria in Zanzibar: a pre-elimination setting. *Malaria journal* **14**, 1-6 (2015).

64. C. Ponce, F. Kaczorowski, T. Perpoint, P. Miailhes, A. Sigal, E. Javouhey, Y. Gillet, L. Jacquin, M. Douplat, K. Tazarourte, Diagnostic accuracy of loop-mediated isothermal amplification (LAMP) for screening patients with imported malaria in a non-endemic setting. *Parasite* **24**, (2017).

65. L. Yu, S. Wu, X. Hao, X. Dong, L. Mao, V. Pelechano, W.-H. Chen, X. Yin, Rapid detection of COVID-19 coronavirus using a reverse transcriptional loop-mediated isothermal amplification (RT-LAMP) diagnostic platform. *Clinical chemistry* **66**, 975-977 (2020).

66. X. Zhu, X. Wang, L. Han, T. Chen, L. Wang, H. Li, S. Li, L. He, X. Fu, S. Chen, Multiplex reverse transcription loop-mediated isothermal amplification combined with nanoparticle-based lateral flow biosensor for the diagnosis of COVID-19. *Biosensors and Bioelectronics* **166**, 112437 (2020).

67. N. Panpradist, E. C. Kline, R. G. Atkinson, M. Roller, Q. Wang, I. T. Hull, J. H. Kotnik, A. K. Oreskovic, C. Bennett, D. Leon, Harmony COVID-19: A ready-to-use kit, low-cost detector, and smartphone app for point-of-care SARS-CoV-2 RNA detection. *Science advances* **7**, eabj1281 (2021).

68. M. G. Rohatensky, D. M. Livingstone, P. Mintchev, H. K. Barnes, S. C. Nakoneshny, D. J. Demetrick, J. C. Dort, G. van Marle, Assessing the performance of a Loop Mediated Isothermal Amplification (LAMP) assay for the detection and subtyping of high-risk suptypes of Human Papilloma Virus (HPV) for Oropharyngeal Squamous Cell Carcinoma (OPSCC) without DNA purification. *BMC cancer* **18**, 1-10 (2018).

69. Z. Yu, W. Lyu, M. Yu, Q. Wang, H. Qu, R. F. Ismagilov, X. Han, D. Lai, F. Shen, Self-partitioning SlipChip for slip-induced droplet formation and human papillomavirus viral load quantification with digital LAMP. *Biosensors and Bioelectronics* **155**, 112107 (2020).

70. K. Yin, V. Pandian, K. Kadimisetty, C. Ruiz, K. Cooper, J. You, C. Liu, Synergistically enhanced colorimetric molecular detection using smart cup: a case for instrument-free HPV-associated cancer screening. *Theranostics* **9**, 2637 (2019).

71. M. Hagiwara, H. Sasaki, K. Matsuo, M. Honda, M. Kawase, H. Nakagawa, Loop-mediated isothermal amplification method for detection of human papillomavirus type 6, 11, 16, and 18. *Journal of medical virology* **79**, 605-615 (2007).

72. R. J. Li, M. G. Mauk, Y. Seok, H. H. Bau, Electricity-free chemical heater for isothermal nucleic acid amplification with applications in COVID-19 home testing. *Analyst* **146**, 4212-4218 (2021).

73. A. H. Buultjens, K. Vandelannoote, L. K. Sharkey, B. P. Howden, I. R. Monk, J. Y. Lee, T. P. Stinear, Low-Cost, Open-Source Device for High-Performance Fluorescence Detection of Isothermal Nucleic Acid Amplification Reactions. *ACS biomaterials science & engineering* **7**, 4982-4990 (2021).

74. Y. Wang, K. Li, G. Xu, C. Chen, G. Song, Z. Dong, L. Lin, Y. Wang, Z. Xu, M. Yu, Low-cost and scalable platform with multiplexed microwell array biochip for rapid diagnosis of COVID-19. *Research* **2021**, (2021).

75. M. Liu, Y. Zhao, H. Monshat, Z. Tang, Z. Wu, Q. Zhang, M. Lu, An IoT-enabled paper sensor platform for real-time analysis of isothermal nucleic acid amplification tests. *Biosensors and Bioelectronics* **169**, 112651 (2020).

76. N. Li, M. Shen, J. Liu, L. Zhang, H. Wang, Y. Xu, J. Cheng, Multiplexed detection of respiratory pathogens with a portable analyzer in a "raw-sample-in and answer-out" manner. *Microsystems & nanoengineering* **7**, 1-10 (2021).

77. M. Zhang, J. Liu, Z. Shen, Y. Liu, Y. Song, Y. Liang, Z. Li, L. Nie, Y. Fang, Y. Zhao, A newly developed paper embedded microchip based on LAMP for rapid multiple detections of foodborne pathogens. *BMC microbiology* **21**, 1-13 (2021).

78. D. Liu, Y. Zhu, N. Li, Y. Lu, J. Cheng, Y. Xu, A portable microfluidic analyzer for integrated bacterial detection using visible loop-mediated amplification. *Sensors and Actuators B: Chemical* **310**, 127834 (2020).

79. J. A. Hambalek, J. E. Kong, C. Brown, H. E. Munoz, T. Horn, M. Bogumil, E. Quick, A. Ozcan, D. Di Carlo, Methylation-Sensitive Loop-Mediated Isothermal Amplification (LAMP): Nucleic Acid Methylation Detection through LAMP with Mobile Fluorescence Readout. *ACS sensors* **6**, 3242-3252 (2021).

80. T. Kuhara, T. Yoshikawa, M. Ihira, D. Watanabe, Y. Tamada, H. Katano, Y. Asano, Y. Matsumoto, Rapid detection of human herpesvirus 8 DNA using loop-mediated isothermal amplification. *Journal of virological methods* **144**, 79-85 (2007).

81. Creating Standard Curves with Genomic DNA or Plasmid DNA Templates for Use in Quantitative PCR. 2003.

82. E. Primiceri, M. S. Chiriacò, F. M. Notarangelo, A. Crocamo, D. Ardissino, M. Cereda, A. P. Bramanti, M. A. Bianchessi, G. Giannelli, G. Maruccio, Key enabling technologies for point-of-care diagnostics. *Sensors* **18**, 3607 (2018).

83. S. C. Tan, B. C. Yiap, DNA, RNA, and protein extraction: the past and the present. *Journal of Biomedicine and Biotechnology* **2009**, (2009).

84. U. Lehmann, C. Vandevyver, V. K. Parashar, M. A. Gijs, Droplet-based DNA purification in a magnetic lab-on-a-chip. *Angewandte Chemie International Edition* **45**, 3062-3067 (2006).

85. X. Shi, C.-H. Chen, W. Gao, S.-h. Chao, D. R. Meldrum, Parallel RNA extraction using magnetic beads and a droplet array. *Lab on a Chip* **15**, 1059-1065 (2015).

86. P. Oberacker, P. Stepper, D. M. Bond, S. Höhn, J. Focken, V. Meyer, L. Schelle, V. J. Sugrue, G.-J. Jeunen, T. Moser, Bio-On-Magnetic-Beads (BOMB): Open platform for high-throughput nucleic acid extraction and manipulation. *PLoS biology* **17**, e3000107 (2019).

87. A. Yamaguchi, K. Matsuda, M. Uehara, T. Honda, Y. Saito, A novel automated device for rapid nucleic acid extraction utilizing a zigzag motion of magnetic silica beads. *Analytica Chimica Acta* **906**, 1-6 (2016).

88. S. Goldberg, Mechanical/physical methods of cell disruption and tissue homogenization. *2D PAGE: Sample preparation and fractionation*, 3-22 (2008).

89. D. W. Burden, Guide to the disruption of biological samples-2012. *Random Primers* **12**, 1-25 (2012).

90. A. A. Yousif, A. A. Al-Naeem, M. A. Al-Ali, Rapid non-enzymatic extraction method for isolating PCR-quality camelpox virus DNA from skin. *Journal of virological methods* **169**, 138-142 (2010).

91. F. H. Biase, M. M. Franco, L. R. Goulart, R. C. Antunes, Protocol for extraction of genomic DNA from swine solid tissues. *Genetics and Molecular Biology* **25**, 313-315 (2002).

92. S. R. Berglund, C. W. Schwietert, A. A. Jones, R. L. Stern, J. Lehmann, Z. Goldberg, Optimized methodology for sequential extraction of RNA and protein from small human skin biopsies. *Journal of investigative dermatology* **127**, 349-353 (2007).

93. E. K. Heiniger, J. R. Buser, L. Mireles, X. Zhang, P. D. Ladd, B. R. Lutz, P. Yager, Comparison of point-of-care-compatible lysis methods for bacteria and viruses. *Journal of microbiological methods* **128**, 80-87 (2016).

94. L. J. Griffiths, M. Anyim, S. R. Doffman, M. Wilks, M. R. Millar, S. G. Agrawal, Comparison of DNA extraction methods for Aspergillus fumigatus using real-time PCR. *Journal of Medical microbiology* **55**, 1187-1191 (2006).

95. C. Gill, J. H. van de Wijgert, F. Blow, A. C. Darby, Evaluation of lysis methods for the extraction of bacterial DNA for analysis of the vaginal microbiota. *PloS one* **11**, e0163148 (2016).

96. J. Buser, A. Wollen, E. Heiniger, S. Byrnes, P. Kauffman, P. Ladd, P. Yager, Electromechanical cell lysis using a portable audio device: enabling challenging sample preparation at the point-of-care. *Lab on a chip* **15**, 1994-1997 (2015).

97. G. Gunaratna, A. Manamperi, S. Böhlken-Fascher, R. Wickremasinge, K. Gunawardena, B. Yapa, N. Pathirana, H. Pathirana, N. de Silva, M. Sooriyaarachchi, Evaluation of rapid extraction and isothermal amplification techniques for the detection of Leishmania donovani DNA from skin lesions of suspected cases at the point of need in Sri Lanka. *Parasites & vectors* **11**, 1-7 (2018).

98. T. Sedlackova, G. Repiska, P. Celec, T. Szemes, G. Minarik, Fragmentation of DNA affects the accuracy of the DNA quantitation by the commonly used methods. *Biological Procedures Online* **15**, 1-8 (2013).